Large-scale, linked drainage systems in the NW European Triassic: insights from the Pb isotopic composition of detrital K-feldspar.

Shane Tyrrell[1]*, Peter D.W. Haughton[1], A. Kate Souders[2], J. Stephen Daly[3] and Patrick M. Shannon[1]

[1]Sand Provenance Centre, UCD School of Geological Sciences, University College Dublin, Belfield, Dublin 4, Ireland

[2]MicroAnalysis Facility, INCO Innovation Centre and Department of Earth Sciences, Memorial University, St. John's, NL A1B 3X5, Canada

[3]National Centre for Isotope Geochemistry, UCD School of Geological Sciences, University College Dublin, Belfield, Dublin 4, Ireland

* Corresponding author (e-mail: shane.tyrrell@ucd.ie)

Words: 6070, References: 50, Tables: 2, Figures: 8

Running head: Palaeodrainage in the NW European Triassic

Abstract: Pb isotopic data from K-feldspars in Middle Triassic (Anisian) sandstones in the Wessex Basin, onshore southwest UK, and the East Irish Sea Basin, some 350 km to the north, show that the same grain populations are present. This indicates that the drainage system (the "Budleighensis" River) feeding these basins originated from the same source/s, most probably the remnant Variscan Uplands to the south. Fluvial and aeolian sandstones have the same provenance, suggesting that if water- and wind-driven sands were originally derived from different sources, this has been obscured through reworking prior to final deposition. Significant recycling of feldspar from arkosic sandstones in earlier sedimentary basins can be ruled out. The provenance data agree with previous depositional models, indicating transport distances in excess of 400 km, with a drainage pattern that linked separate basins. This supports the idea that the regional fluvial system was driven by topography and episodic flooding events of sufficient magnitude to overcome evaporation and infiltration over hundred's of kilometres. Importantly, this drainage system appears to have been isolated and independent from those operating

contemporaneously to the northwest of the Irish and Scottish massifs, where the remnant Variscan Uplands apparently exerted no influence on drainage or sand supply.

The Southern UK and offshore Ireland Triassic succession, comprising the Early – Middle Triassic (Olenekian – Anisian) Sherwood Sandstone Group (SSG) and the Middle – Late Triassic (Ladinian – Norian) Mercia Mudstone Group, represents the deposits of large-scale endorheic drainage systems that accumulated in the arid to semi-arid interior of the Pangaean Supercontinent. Infilling a series of wide, extensional rift basins, the distribution and depositional style of these successions is well constrained, both onshore and offshore UK and include ephemeral fluvial, alluvial and playa lacustrine with sub-ordinate aeolian facies. The Variscan Uplands of west and central Europe are thought to have exerted a strong control on drainage evolution, resulting in large-scale (> 300 km), south-to-north flowing rivers (i.e. the 'Budleighensis' river system; Wills 1970; Audley-Charles 1970; Warrington & Ivimey-Cooke 1992) which fed a series of sedimentary basins and terminated in playa lake environments. It has also been established that the distribution of sedimentary facies in the Triassic basins was controlled by a complex interplay of climate and tectonics (Ruffell & Shelton 1999). Dispersal of clastic material from the uplands into the basins was likely driven by both topography and by climate, and was particularly influenced by periodic (perhaps seasonal) variations in precipitation (McKie and Williams, 2009). Palaeomagnetic data suggest that this area of NW Europe lay between 15 and 25° N and was influenced by SW-directed subtropical trade winds giving rise to general semi-arid conditions (McKie and Williams, 2009) but with an annual summer monsoon (Kutzbach & Gallimore 1989; Szulc 1999; Preto *et al.* 2010). Cyclic variability in sedimentation in the European Triassic (Meadows & Beach 1993; Bourquin *et al.* 2009) suggests that large scale fluvial systems were more active during phases of increased precipitation (McKie & Williams 2009). The majority of this precipitation likely fell on the high ground and especially on the remnant Variscan Uplands, as this would have been the first significant high ground encountered by the monsoonal weather systems originating from the south. Flooding was, therefore, likely an annual occurrence, driving transport of clastic material from the uplands into the hinterland basins and beyond.

The term 'Budleighensis' river was first proposed to account for the deposition of thick, regionally-significant, fine to medium-grained, red-bed sandstone-dominated facies of Triassic (Olenekian – Anisian) age across south, central and north-east England (Wills 1970; Audley-Charles 1970). Interpreted to flow from south to north, and with deposits apparently related to this system encountered in the Wessex, Knowle, Worcester, Stafford, Cheshire and East Irish Sea basins (and perhaps further north into the Solway and Ulster basins) (Figure 1, 2), it is among the better documented large-scale, climate-controlled fluvial systems of the Triassic. The topographically

significant Variscan Uplands to the south are suggested to be the source for these sandstones (Wills 1950; Fitch *et al.* 1966). However, the source areas of these sedimentary rocks have not been explicitly demonstrated.

Various approaches have been applied to determine the provenance of Early – Middle Triassic successions in central Europe (e.g. Koppen and Carter 2000), in the North Sea (Mearns *et al.* 1989; Knudsen 2001; Preston *et al.* 2002), in basins west of Ireland (Tyrrell *et al.* 2007) and west of Shetland (Morton *et al.* 2007; Tyrrell *et al.* 2009) but provenance research specifically on the 'Budleighensis' system has been limited. Previous provenance work in the Wessex Basin mainly focussed on the lithological comparison of clast assemblages in conglomeratic horizons (especially in the Budleigh Salterton Pebble Beds, Smith 1990; Smith & Edwards 1991), which do not necessarily share the same provenance as the finer grained sandstones that dominate higher in the succession and that are the focus of this study. Nonetheless, these petrographic studies identified detritus of Variscan granites and gneisses of likely Cadomian affinity, both sourced from northern France. Fitch *et al.* (1966) utilised detrital muscovite ages to demonstrate the predominance of Variscan-aged detritus in the Cheshire Basin. Detailed analysis of heavy mineral assemblages in feldspar-rich sandstones from the East Irish Sea Basin (Mange *et al.* 1999) was used to correlate barren strata. Mange *et al.* (1999) argue that local input, particularly from the Welsh Massif, was significant, mostly from reworked metasedimentary and sedimentary rocks. There are also components (especially tourmaline) which indicate a southern, Variscan Upland, source, whereas zircon could not be linked to a specific provenance. Notably, the source areas suggested by Mange *et al.* (1999) cannot account for the abundance of K-feldspar in these sandstones.

The sandstones targeted in this study form a regionally important aquifer and a proven reservoir for hydrocarbons in a number of sedimentary basins in the area, including the Wessex and East Irish Sea basins (McKie *et al.* 2007; Meadows and Beach 1993). Provenance analysis of the drainage system supplying these sands is important because its scale is relatively poorly constrained (<200 km or >500 km?) and it is uncertain as to how far it extends northward, possibly beyond the East Irish Sea Basin and into the Solway (Brookfield 2004) and/or Ulster basins. Furthermore, it is unclear to what extent these separate basins drained internally or whether the envisaged large-scale fluvial system was through-going within the array of sedimentary basins from the Wessex Basin northward to the East Irish Sea Basin. There are also uncertainties as to the relative contributions of axial (i.e. the Variscan Uplands) and more local transverse sources (e.g. the Welsh Massif, the London-Brabant High) and the potential contrasts in sources of fluvial and aeolian sediment. Moreover, it is not certain how or if these systems are related to contemporaneous drainage systems operating further to the north and west in the

Atlantic Margin basins. Although it was originally envisaged that Triassic drainage systems in the Atlantic Margin basins were derived from and controlled by the Variscan Uplands to the south (e.g. in the Slyne Basin, Dancer 2005), recent work has shown this not to be the case (Tyrrell *et al.* 2007; McKie & Williams 2009; Redfern *et al.* 2010). In terms of the broad regional Triassic system, therefore, it is important to recognise how, and to speculate why, these systems may differ. In broader terms, these types of provenance studies help constrain the pattern of rifting within this part of the Pangaean Supercontinent, as the uplift and availability of specific source domains is recorded in the detrital archive.

In petrographic terms, the nature of these sandstones poses some additional questions. It is unclear how the interaction of topography, tectonics and climatic factors can produce extensive regional spreads of sandstones such as those seen in the Triassic in NW Europe. The origin and genesis of these widely-dispersed, texturally mature, yet mineralogically sub-mature (arkosic), sandstones is believed to result from the complex interplay of climate and tectonics (Ruffell & Shelton 1999; Brookfield 2004). Establishing the provenance of these sandstones, especially with a method that utilises a key framework component (i.e. K-feldspar), allows for a better understanding of these processes.

The Pb-in-K-feldspar provenance tool is particularly applicable to addressing some of the above issues, especially given the feldspathic nature of the Triassic sandstones in these basins. Recent studies have demonstrated the value of the Pb isotopic composition of detrital K-feldspar as a regional scale sand provenance tool (Tyrrell *et al.* 2007, 2009, 2010; Clift *et al.* 2008). It has been shown that K-feldspar retains the signature of its source despite erosion, transport and diagenesis (Tyrrell *et al.* 2006). The continental crust exhibits sub-orogenic scale (~100 km) variations in Pb isotopic composition and potential sourcelands can thus be characterised on a scale appropriate to that of major drainage systems. Furthermore, the Pb isotopic signature of a granitic or gneiss does not vary with depth, hence K-feldspar with the same distinct Pb signature will always be supplied for a discrete source area regardless of the erosion level. The method involves *in situ* Pb isotopic analysis of individual detrital K-feldspar sand grains using laser ablation multi-collector inductively-coupled plasma mass spectrometry (LA-MC-ICPMS) preceded by detailed imaging (Backscatter electron (BSE) and cathodoluminescence (CL) imaging) so that heterogeneities (e.g. inclusions, alteration) can be avoided. The use of ion counters to measure Pb ion beams means that data can be retrieved at a spatial resolution (~30 μm laser spot sizes) similar to that achieved using the ion microprobe technique, but with better analytical precision (Tyrrell *et al.* 2010). Using LA-MC-ICPMS to analyse the Pb isotopic signal means the data can be acquired rapidly and relatively inexpensively and the technique requires only a previously-

imaged, thick polished section, thereby retaining the grain context within the sedimentary rock sample.

One of the major advantages of the Pb K-feldspar provenance tool is that, in contrast to provenance approaches that utilise signals in robust grains (e.g. U-Pb zircon), it provides a means of assessing first-cycle sand-grain provenance. Furthermore, where it occurs as a significant framework component (~20% modal abundance), K-feldspar must presumably be more representative of the source area than relatively minor components such as zircon which typically make up << 1% of the mode. In these circumstances, K-feldspar can be a proxy for the source of a large portion of the detrital quartz as there is a reasonable probability both minerals are derived from the same source/s. As fresh detrital K-feldspar is unlikely to survive more than one sedimentary cycle, these grains can be tracked back directly to their basement source, allowing the scale and geometry of the drainage system to be constrained. These types of insights can improve prediction of reservoir sandstone distribution and quality in the subsurface. Importantly, there is much published Pb data from potential basement source areas in the North Atlantic Region with which detrital data can be compared. In this study, additional basement data were collected to provide further constraints on possible sources.

This study is specifically focussed on Middle Triassic sandstones. Although there are uncertainties with the definitive ages within the Triassic system due to the scarcity of biostratigraphic markers, Rhyncosaurs provide constraints on the Otter Sandstone Formation (Hounslow and MacIntosh 2003) in the Wessex Basin and palaeomagnetic data helps constrain the age of the Ormskirk Sandstone Formation in the EISB (Meadows 2006). These sandstones units are considered to correspond to the upper part of SSG, are very likely of Anisian age and are both near contemporaneous (Figure 1, 2). Both units lie directly above a distinct and widely recognised discontinuity, namely the Hardesgan Unconformity (McKie & Williams 2009; McKie & Shannon 2011). Correlated well log data illustrate that Otter Formation sandstones comprise a relatively thin succession within the Wessex Basin, but their equivalents are thicker in the basins to the north (Figure 2; McKie & Williams 2009). This thickening is not as significant as that seen in the Early-Middle Triassic sandstones (Lower SSG) where the increased accommodation space to the north is likely due to a combination of differential subsidence and tectonism. In the EISB, the Ormskirk Formation sandstones are interbedded with thin mudstones and mud-prone sandstones, likely of playa lake and damp aeolian sandsheet origin, and may reflect the onset of termination of the drainage system (McKie & Williams 2009).

Methods:

Sampling and petrography:

Cores from four East Irish Sea Basin wells (Figure 1) were sampled at the Department of Energy and Climate Change (DECC) core store, Edinburgh, UK. The choice of EISB sandstone samples was guided by extensive sedimentary logging carried out by Meadows (2004). The sampling strategy was designed to target the same range of stratigraphy and facies from four wells penetrating the Ormskirk Sandstone Formation. Coastal outcrops of Budleigh Salterton Pebble Beds and the overlying Otter Sandstone Formation were also sampled at Budleigh Salterton in the Wessex Basin. New basement samples were collected in the field, or, in the case of granites from southwest UK and northern France, selected from petrographic collections based at the UCD School of Geological Sciences (see table 2 for locations). Thin sections of all samples were examined using standard optical petrography.

Backscatter electron and cathodoluminescence imaging:

After initial petrographic assessment, sections of ~300μm thickness were prepared from which K-feldspar grains were selected and imaged using backscatter electron (BSE) and cathodoluminescence (CL) at the Electron Microprobe Laboratory, Geowissenschaftliches Zentrum, Göttingen, Germany. Further BSE images K-feldspars were collected using a Hitachi TM-1000 desktop scanning electron microscope at the School of Geological Sciences, University College Dublin, Ireland.

Pb analysis:

Pb, U and Th concentrations were determined at the Microanalysis Facility, InCo Innovation Centre, Memorial University, Newfoundland (MUN), using an ELEMENT ICPMS connected to a Geolas 193nm Excimer laser. Pb isotopic analyses were carried out both at MUN and at the National Centre for Isotope Geochemistry (NCIG) at UCD, Dublin, using NEPTUNE MC-ICPMS instruments. A New Wave 193nm excimer laser was employed to ablate the target grains at NCIG.

Two different collector configurations were used during analysis. An ion counter collector configuration was implemented at MUN, allowing Pb analysis from ~30 μm laser ablation pits, which is only slightly larger than spot sizes used to collect Pb isotopic data using secondary ion mass spectrometry (SIMS) (e.g. Clift *et al.* 2008), but with much lower errors and better reproducibility. A Faraday collector array was utilised at the NCIG, where tracks of <150 μm with a spot size of 75 μm were ablated in preference to single spots. The larger volume of material was ablated when using the Faraday collectors, as these are not as sensitive as the ion counters. Repeat analyses of the same grains replicated the initial data within error (Table 1).

The analytical technique is described in more detail in Tyrrell *et al.* (2009, 2010). ^{204}Pb, ^{206}Pb, ^{207}Pb and ^{208}Pb were measured. ^{202}Hg was also measured during analysis in order to correct for isobaric interference of ^{204}Hg on ^{204}Pb. In the case of the Faraday collectors, ^{203}Tl and ^{205}Tl were measured and utilised in the standard-sample bracketing fractionation corrections. For both collector configurations, these instrumental mass bias corrections were based on isotopic ratios measured in either standard glasses BCR2g or NIST 612. Analytical uncertainties (2σ on ^{206}Pb/^{204}Pb) are <0.1%. Within each analytical run, standard glasses, including NIST 612 and BCR2g and samples of Shap Granite feldspar (which has a well-characterised and narrow range of Pb isotopic composition) were run as unknowns in order to verify the data reduction. The values obtained for these "unknown knowns" standards and the Shap Granite K-feldspar are within error of published values, which have been obtained through isotope dilution thermal ionisation mass spectrometry.

Results

The sampled arkosic sandstones are generally medium-grained and well-sorted with feldspar contents (dominantly K-feldspar) varying between 12.5% and 22.5%. The sandstones contain patchy dolomite cements, authigenic quartz and K-feldspar overgrowths. SEM imaging of K-feldspars show a variety of inclusions, dominantly albitic lamellae, albitic veins and quartz, and often display areally restricted alteration. This alteration usually comprises discrete zones of the grains which have undergone albitisation, but less frequently the K-feldspar has been further altered such that only a skeletal framework remains. In any case, altered zones were avoided during laser ablation. Rounded K-feldspar grains are common, both in fluvial and aeolian sandstones, and there is no obvious association between grain morphology and sedimentary facies. Authigenic K-feldspar overgrowths are common in all the sampled sandstones, often modifying the primary detrital K-feldspar grain shape (Figure 3). CL imaging proved particularly useful in indicating the overgrowths, with the authigenic component often picked out by a darker CL response in contrast to the bright luminescence of the original detrital grains (Figure 3B). Although the overgrowths were not wide enough to analyse, they were avoided during analysis in case their Pb signal differed from that in the detrital grains.

The Pb concentration (where analysed) and isotopic composition of 187 individual K-feldspar grains from 20 samples are shown in Table 1. This dataset comprises analyses of 73 K-feldspars from the Ormskirk Sandstone Formation in four wells (110/14-3; 110/13-5; 110/8a-5; 110/2-6) in the East Irish Sea Basin (locations shown in Figure 1) and 114 K-feldspars from the Otter Sandstone Formation and 2 K-feldspar crystals from a clast of feldspar porphyry from the Budleigh Salterton Pebble Beds (BSPB), both from coastal outcrops in the Wessex Basin. Ninety

one of the 114 K-feldspars analysed from the Otter Sandstone Formation were obtained using the Faraday collector configuration (see above). This included the re-analysis of several grains, the results of which replicated the initial data (see data marked “repeat” in table 1).

Where measured, Pb concentrations of K-feldspar grains varied between 5 and 200 ppm (mean = 75 ppm). U and Th concentrations for measured grains and are typically < 0.01 ppm. A small number of grains had U and Th concentrations in excess of 0.5 ppm, but the vast majority had sufficient U or Th to require corrections to the common Pb signature for radioactive decay. There is no discernable link between the Pb, U and Th concentration and the isotopic composition of the grains. Pb isotopes from the K-feldspars are generally radiogenic with $^{206}Pb/^{204}Pb$ in the range 17.124 to 18.561 (mean = 18.136) and $^{207}Pb/^{204}Pb$ in the range 15.289 to 15.849 (mean = 15.591). The more radiogenic grains are more abundant, with the most dense grouping in the $^{206}Pb/^{204}Pb$ range of 18.1 to 18.5 (Figure 4).

Detrital K-feldspar data can be compared directly with Pb data from basement rocks in NW Europe, comprising both K-feldspar and whole rock analyses. These comparative datasets are compiled from published work and are supplemented with new basement data (Table 2). Published data come from numerous sources, summarised in Tyrrell *et al.* (2006, 2007, 2009, 2010). New data comprise analysis of K-feldspars in granitic rocks from northern France, south east Ireland and the south east UK and Carboniferous sandstones from NW Ireland. Rocks from northern France were analysed in order to verify the Pb isotopic signature of K-feldspar from Variscan Granites in this area and to constrain that of older granites and granitic rocks in the region. Data from Variscan Granites in Normandy and Brittany largely agree with published values from Vitrac *et al.* 1981, although they form a broader range (Figure 5A, 5B). However it should be noted that although the range of new data includes a 2σ error, the errors are not shown for the previously published data. Pb K-feldspar analyses of Cadomian-aged granites from the same region yield less radiogenic Pb than the Variscan granites (Figure 5A, see discussion below). Analysis of Variscan Granite from Cornwall (the Lands End Granite) yields a slightly more radiogenic signature than the pene-contemporaneous granites from northern France (Figure 5A). Further new analyses from granitic rocks from south east Ireland constrain the Pb isotopic signature of the Carnsore and Leinster Granites and a granitic vein cutting the Rosslare Complex (Figure 5C). Although these could potentially be a source of K-feldspar themselves, especially for the EISB K-feldspars, they also may be a reasonable proxy for the Pb isotopic signature of the Welsh Massif (see discussion below). It is worth noting that although the Caledonian-aged Leinster Granite has a Pb isotopic signature which is almost identical to other Caledonian granites along structural strike, south of the Southern Uplands (i.e. the Shap Granite, Figure 5C, D), the Carnsore Granite (also Caledonian in age) has a less radiogenic signature and has more

in common with the Cadomian granite of northern France (Figures 5C, A). The Pb isotopic composition of detrital K-feldspar from arkosic Lower Carboniferous sandstones (Mullaghmore Sandstone Formation) in NW Ireland was analysed (Figure 6) in order to constrain potential second-cycle K-feldspar sources on the Irish Massif.

Discussion:

The 'Budleighensis' river system:

The Pb isotopic composition of detrital K-feldspar grains in contemporaneous Middle Triassic sandstones from 1) the Ormskirk Sandstone Formation from exploration well cores in the EISB (offshore East UK); and 2) outcrops of Otter Sandstone Formation in the Wessex Basin (onshore southwest UK) broadly show the same ranges of Pb isotopic composition (Figure 4C). There is a subtle difference in that, although the range of $^{206}Pb/^{204}Pb$ is almost identical between the two sandstone units, the $^{207}Pb/^{204}Pb$ range and average is slightly lower in the Wessex Basin sandstones (Figure 4A, B). This variation is small and, although it might reflect differences in the relative proportions of grains derived from each contributing source areas, it does not suggest a significantly different provenance (Figure 5). The suggestion of common source areas for both these sandstone units indicates that the drainage system supplying the two basins was linked, suggesting they lay along the same regional sand dispersal path which threaded northward through the intervening basins and sub-basins.

The most likely source (i.e. the best fit given the range of data) for the bulk of the K-feldspar grains are granites and granitic rocks of Variscan and older age comprising the remnant Variscan Uplands to the south, especially those from northern France (Brittany and Normandy; Figure 5A) and, to a lesser extent, the French Massif Central and the Pyrennes (Figure 5B). There is also input from more local sources on the Cornubia Massif, though the data indicate this is a relatively minor component compared to the contribution from northern France sources (Figure 5A). However, data are from one granite (the Land's End granite) and there may have been a larger contribution from other granites such as the volumetrically significant Dartmoor Granite for which Pb isotopic data are not yet available.

New Pb basement data suggests that the less radiogenic Pb K-feldspar (i.e. $^{206}Pb/^{204}Pb < 18$) is likely derived from Precambrian granites and gneisses within the Variscides (Figure 5A). These rocks, either associated with the Cadomian orogeny or of older ambiguous origin, comprise part of modern Brittany, Normandy and the Channel Islands. Although there are data from only one rock unit of this affinity (the Carolles Granite) it is postulated that basement of Cadomian and pre-

Cadomian affinity was partly/wholly reworked on a regional scale to produce Variscan granites, so the Pb component in the later granites was inherited from early basement (Vitrac *et al.* 1981). The reworking of Cadomian basement Pb into Variscan granites is also recorded in central Europe (Klötzli *et al.* 2001). This agrees with the new data, where Pb in Cadomian K-feldspar is less radiogenic than its Variscan successor, and hence these rocks are an appropriate source for the less radiogenic populations in the Triassic detrital record.

The Pb isotopic signature of the authigenic K-feldspar overgrowths is not known and it remains unclear how these might relate to that of the detrital grains. An understanding of these could provide constraints on the nature and source of early pore fluids. With smaller spot sizes and optimised ICPMS conditions it should be feasible in future to measure the Pb isotopic composition of these thin grain coating rims.

These data suggest minimum drainage length-scales in excess of 400 km for the 'Budleighensis' river system. This is in agreement with published palaeoflow data and with palaeogeographic reconstructions for the period (Audley-Charles, 1970). However, sources from farther south cannot be ruled out and it is consistent with the Pb data that some grains have been transported from the Pyrenees or the Massif Central. This would imply drainage scales in excess of 800 km.

There are some ambiguities within the data which prevent the ruling out of certain sources. For example, basement data from Southern Uplands granites partially overlap with Variscan Pb domains. Hence, feldspar data from the WB corresponds well with that from Southern Uplands Granites (Figure 5D), but it is extremely difficult to envisage a process where this could be a major source for sandstones in the Wessex Basin. This 'sourcing' would also conflict with the wealth of published palaeocurrent data indicating northward transport. However, the Southern Uplands could reasonable contribute a minor source for sand in the more proximal EISB. In addition, feldspar data from the EISB partially overlaps with the range of Shap Granite K-feldspar (Figure 5D). This, therefore, is a possible source for some of the sand in the EISB, but the lack of significant grains from a broader area of Northern England or the Scottish Massif suggests this area was, at most, a minor contributor of K-feldspar.

There are no comparative basement Pb data available from the Welsh or the London-Brabant Massifs, therefore it remains uncertain to what extent these areas could be a source for clastic detritus during the Triassic. There is little evidence to suggest that the London-Brabant Massif comprised significant sources of K-feldspar. New Pb K-feldspar basement data from Caledonian granites (Carnsore and Leinster Granites), and a mylonitised granitic vein (cutting the Rosslare Complex, a terrane of Avalonian affinity, correlated with the Monian of NW Wales (Gibbons and

Horak 1996)) and published galena data from the Irish Massif (Figure 5C) are likely a reasonable proxy for the Pb isotopic basement composition of the Welsh Massif as these southern Irish domains extend along strike north-eastward. Although there is some overlap between these basement data and the detrital data, the same range of data is not seen in the detrital dataset (Figure 5C), indicating that the Welsh Massif was likely only a minor source for the K-feldspar grains in the EISB and WB. There are also grains with Pb isotopic compositions that outlie the range of characterised Variscan or Cadomian K-feldspar (Figure 5E) and do not appear to correspond to any other specific source. These grains may represent uncharacterised Variscan, Cadomian or a more minor contributory basement source and their presence supports the preferred models of palaeodrainage which envisage detrital contributions from a wide catchment via an extensive tributary system.

The work of Mange *et al.* (1999) concluded that a significant fraction of the heavy mineral detritus in the Ormskirk Sandstone Formation was recycled, speculatively from the Welsh Massif. It is sensible to assume that a portion of the detrital zircon present was also recycled from older sedimentary successions. Geochronological data from zircons in these sandstones are likely, therefore, to have yielded a "mixed" and non-unique range of ages, due to the incorporation of recycled and/or inherited zircon from the numerous igneous, sedimentary and meta-sedimentary sources which may have been available. Its is possible to imagine such diverse sources for recycled zircon as Lower Palaeozoic meta-sedimentary successions on the Welsh Massif, Old Red Sandstone and Culm-facies equivalents from Cornubia, or from Upper Carboniferous sandstones from the Pennine Basin. It would be extremely challenging to unravel this potential mix of contributors, especially as it would likely be impossible to distinguish first cycle from polycyclic material. However, it is worth noting that the modal abundance of K-feldspar in these Triassic sandstones (between 12.5 and 22.5%) implies that lithologies with high K-feldspar contents (granites and gneisses) must have supplied a significant portion of the sand. Rocks with little or no K-feldspar must also have contributed – at the very least contributions from the country rocks surrounding the granitic sources would be anticipated and these, being dominantly sedimentary and metasedimentary in nature, are the likely sources for the recycled components recognised by Mange *et al.* (1999). A more rigourous methodology, incorporating a multiproxy approach, may enable recycled components to be distinguished and quantified, especially if tailored such that signals in both stable and more labile components are interrogated. Preliminary work (Tyrrell *et al*. 2009) has shown that an integration of the Pb-K-feldspar and zircon geochronological techniques can aid in the recognition of recycled components, and consequently can lead to an improved understanding of palaeodrainage.

K-feldspar grains from aeolian and fluvial facies in the EISB cannot be distinguished on the basis of their Pb isotopic compositions (Figure 4D). Therefore, if there were different input points associated with different transport mechanisms into the basin/s (or into sediment storage areas adjacent to the basin), this information has been lost through reworking and mixing of this signal by the last transport prior to deposition. Furthermore, as noted above, rounded feldspar grains of likely aeolian origin are common within the fluvial sandstones of the Otter Sandstone Formation. These phenomena are perhaps expected given that aeolian sediments will be reworked by fluvial mechanisms during wet periods and *vice-versa* during dry periods and have been described in the Triassic Helsby Sandstone Formation in the Cheshire Basin (Mounteney and Thompson 2002). This is therefore in agreement with models of Triassic climate which evoke an annual monsoon and associated flooding (see above; (Kutzbach & Gallimore 1989; Szulc 1999; Preto *et al.* 2010). It would be anticipated that monsoon weather systems, pulled from the south during summer continental heating and carrying moist air from Tethys, would shed much of their precipitation upon reaching the remnant uplands resulting in large-scale north-directed flooding (McKie & Williams 2009). Such reworking, associated with flooding and wet-dry fluctuations, is observed in the evolution of modern monsoon-influenced drainage systems such as the Indus (Alizai *et al.* 2011).

It has been previously suggested that K-feldspar in the EISB Triassic could have been recycled and supplied from Upper Carboniferous sandstones (the Millstone Grit Group of the Pennine Basin) cropping out to the east of the basin (Meadows 2004, 2006). However, published Pb analyses of K-feldspars from these sandstones (Tyrrell *et al.* 2006) show that they contain a distinct bimodal distribution of grains, including an unradiogenic population (ultimately linked to a Lewisian or Greenland source) which is not found in the EISB Triassic (Figure 6). This suggests that the Millstone Grit Group in the Pennine Basin 1) was not available as a source for sediment in the EISB during the Triassic; 2) was eroding at this time but sediment was "trapped" in the hangingwalls adjacent to the eastern basin-bounding faults; or 3) contributed detritus but the K-feldspar component did not survive a second sedimentary cycle.

Implications for regional palaeodrainage and sandstone distribution:

The provenance interpretation presented in this paper indicate that the sand carried by the 'Budleighensis' river system was dominantly sourced from the Variscan Uplands (Figure 7). This interpretation supports the original drainage models based on sedimentology and palaeocurrent data (Wills 1950; Wills 1970; Audley-Charles 1970; McKie & Williams 2009). Other regional basement highs, such as the Welsh and Cornubia massifs appear to make more minor contributions.

The drainage directions within the Budleighensis system contrast with those interpreted from feldspar provenance data in Triassic sandstones from basins west and north of the Irish and Scottish Massifs. It has been demonstrated (Figure 6) that K-feldspar grains from apparent SSG equivalents in the Atlantic Margin basins (including data from the Corrib Gasfield in the Slyne Basin, from the Foula Formation, Strathmore Field in the Faeroe-Shetlands Basin and from the Dooish Gas Condensate accumulation on the eastern margins of the Rockall Basin, which, it should be noted, is of uncertain age) comprise unradiogenic Pb and there are no grains which could have been derived from the Variscan Uplands or from any southern source. This suggests no discernable Variscan influence in these areas, and grain populations are dominantly derived from Archaean and Proterozoic rocks in Greenland, NW Scotland, various now semi-obscured or poorly characterised basement highs in on the present continental shelf and possibly from Grenville-affinity rocks from eastern Canada (Tyrrell *et al.* 2007, 2009, 2010; Redfern *et al.* 2010). McKie & Williams (2009) envisage southern derivation directions for SSG equivalents hosting the Corrib Gasfield in the Slyne Basin. This interpretation is in agreement with palaeoflow directions suggested by orientated core (Dancer *et al.* 2005). These interpretations do not consider the significance of K-feldspar grains of Archaean affinity in these sandstones which is strongly indicative of ultimate sand dispersal and input from a northern or northwestern source. However, it is possible to reconcile both datasets, with the provenance data indicating the orientation of the transport system into the Slyne Basin, and the palaeocurrent data recording the orientation of drainage system within the confines of the basin (Figures 7, 8).

This change in dominant drainage direction suggests that the Irish and Scottish Massifs (south of the Great Glen Fault; Figure 7) divide areas draining different catchments during the Early to Middle Triassic. There is currently no K-feldspar provenance data from Ormskirk Sandstone Formation equivalent rocks in the Solway or Ulster basins; hence it is not possible to assess or limit the potential dispersal of Variscan detritus northward beyond the EISB. Interestingly the Ulster Basin appears to thread through and link between the two areas with contrasting drainage regimes (Figure 7, 8). Intriguingly, although the Irish and Scottish massifs appear to act as drainage divides separating systems influenced by and independent from the Variscan Uplands, Pb data from crystalline basement comprising these massifs are insignificant contributors of K-feldspar detritus to either the Atlantic Margin basins (Tyrrell *et al.* 2007, 2010) or to the Budleighensis system (Figure 7, 8). Furthermore, new Pb-in-K-feldspar data from arkosic sandstones of Visean age within the Irish NW Carboniferous Basin (Mullaghmore Sandstone Formation), onshore northwest Ireland, show similar grain populations to those seen in the Serpukhovian-Bashkirian of the Pennine Basin (i.e. they have a bimodal distribution of grains sourced from Archaean – Palaoproterozoic rocks and more proximal Caledonian Granites; Figure

6). These data rule out recycling of K-feldspars into the Atlantic Margin basins from older Carboniferous sandstones on the Irish Massif. In overall terms, therefore, these data suggest that, although the Irish and Scottish Massifs were of sufficient relief to form a barrier to evolving drainage, they remained topographically subdued such that precipitation on, and ensuing associated clastic transport from, these areas was minimal. It could have been the case that the interior was too arid for these areas to be significant sources, with sediment dispersal relying on runoff from the wetter catchments outside the arid interior. This would agree with palaeogeographic and climate models for these areas during the Middle Triassic (Naylor & Shannon, 2011). Alternatively, these areas may have been buried beneath now-eroded sedimentary rocks so as not to have been available as a source for K-feldspar-bearing siliclastic sediments during the Triassic. It is possible that there were significant uplands, but that these dominantly comprised carbonates. However, apatite fission track data (Allen *et al.* 2002) suggest low denudation rates during the Triassic and similar data from the Scottish Massif suggests that significant post-Caledonian uplift did not take place until the Cenozoic (Lewis *et al.* 1992; Hall & Bishop 2002), supporting the idea that these areas remained relatively tectonically quiescent and topographically subdued during much of the early Mesozoic.

It is clear that climate and topography played an important role in sediment dispersal and mixing, but these must have also impacted on sediment release rates. In the envisaged arid environment, low humidity and presumed minimal biogenic activity would result in slow rates of chemical weathering, as suggested by the overall abundance of K-feldspar in the preserved sedimentary products. Mechanical weathering was most likely the dominant process of rock disaggregation. Sediment can be 'stored' and 'pre-sorted', perhaps in areas more proximal to their ultimate source (e.g. as alluvial fans), prior to ultimate deposition (Figure 8). Alternatively, the textural maturity may simply be due to repetitions of aeolian winnowing and fluvial transport during downstream migration of sediment. Dryland systems typically show the progressive sorting producing the mineralogically sub-mature, texturally mature sandstones ubiquitous in both the Lower and Middle Triassic basins of NW Europe.

Conclusions:

K-feldspar sand grains in Middle Triassic sandstones in the Wessex and East Irish Sea basins appear to share the same sources, indicating that the drainage system supplying these sands was through-going and extended northward from the SW England to offshore North Wales. The sand grains were likely derived from the Variscan Uplands to the south, implying drainage length scales in excess of 400 km. Populations are mixed at thin section scale and different facies display the same populations, perhaps indicating that some or possibly all of the sediment was

mixed and reworked by fluvial and/or aeolian processes and accumulated in intermediate storage areas prior to final deposition. These observations agree with the current understanding of Triassic palaeogeography and climate models, where both topography and flooding associated with an annual monsoon are thought to have been responsible for the transport of sediment from the uplands. This combination of processes can also account for the overall textural maturity and mineralogical sub-maturity of the sandstones. Comparison with K-feldspar provenance data from Atlantic Margin basins show that the latter sandstones have a different provenance, were dominantly supplied from Archaean and Proterozoic rocks from the north and west, and that there was no input from the Variscan Uplands. The Triassic K-feldspar provenance data collected to date from all basins in the region indicate the presence of two drainage domains (the 'Budleighensis' and the Atlantic Margin basins), separated by a NE-SW oriented drainage divide. The drainage divide comprised the Irish-Scottish massifs and, although these areas were of sufficient topography to act as a barrier to evolving drainage, they themselves were not a significant source of K-feldspar detritus. Carboniferous arkosic sandstones from the Irish Massif and from the Pennine Basin, Northern England can also be ruled out as sources in both drainage regimes, supporting the idea that detrital K-feldspar in sandstones cannot readily survive reworking and is, therefore, likely first-cycle detritus.

ST is funded by the Department of Communications, Energy and Natural Resources under the National Geoscience Programme 2007-2013 (Griffiths Geoscience Awards). This research forms part of a larger study funded by a Science Foundation Ireland Research Frontiers Programme grant (GEO029) awarded to PDWH. The National Centre for Isotope Geochemistry (NCIG), Dublin, is a joint venture of UCD, Trinity College Dublin and University College Cork, and was funded mainly by Science Foundation Ireland. Mike Tubrett and Paul Sylvester (Microanalysis Facility, Memorial University, Newfoundland, Canada) are thanked for assistance with ICPMS. Dick Sutherland (DTI core store, Edinburgh, UK) is acknowledged for facilitating core sampling. Andreas Kronz (Electron Microprobe Laboratory, Geowissenschaftliches Zentrum, Göttingen, Germany) is thanked for assistance with BSE and CL imaging and EMPA. Tom Culligan (UCD) is thanked for skilful thin section preparation. Two anonymous reviewers are thanked for constructive and helpful comments and suggestions which improved the manuscript.

Figure 1: Schematic palaeogeographic reconstruction of the Middle Triassic (right) after Scotese 2002; Eide 2002; McKie & Williams 2009; Bourquin *et al.* 2011; McKie & Shannon 2011) showing the distribution of massifs and sedimentary basins with summarised Triassic stratigraphy of some NW European basins (left, after McKie & Williams 2009, Tyrrell *et al.* 2010). Also shown are the

553 locations (geographic and stratigraphic) from which Pb K-feldspar provenance data have been
554 obtained, and a map of the East Irish Sea Basin (EISB; inset; after Meadows 2004) showing the
555 location of wells sampled in this study. AM = Armorican Massif; CM = Cornubia Massif; FC =
556 Flemish Cap; HP = Hebridean Platform; IM = Irish Massif; LB = London-Brabant High; PH =
557 Porcupine High; RB = Rockall Bank; SM = Scottish Massif; SP = Shetland Platform. ChB =
558 Chesire Basin; CNB = Central North Sea Basin; CSB = Celtic Sea Basins; EISB = East Irish Sea
559 Basin; FSB = Faeroe Shetland Basin, NNB = Northern North Sea Basin; RBa = Rockall Basin; SB
560 = Slyne Basin; SNB = Southern North Sea Basin; WB = Wessex Basin; WoB = Worcester Basin;
561 ggf = Great Glen Fault.
562
563 **Figure 2:** Stratigraphic panel for the Middle - Upper Triassic from the Wessex Basin northward
564 through the East Irish Sea Basin and into the Ulster Basin adapted from McKie & Williams (2009)
565 and based on their correlation of 10 wireline logs. The datum is the top Triassic. The line of
566 section is shown on Figure 1.
567
568 **Figure 3:** Backscatter electron (A, C, D) and cathodoluminescence (B) images of K-feldspar
569 grains from East Irish Sea and Wessex basins illustrating, A) authigenic overgrowths on K-
570 feldspar which are only visible in CL (B), modifying the primary rounded grain shape; C)
571 authigenic overgrowth on K-feldspar grain (from Wessex Basin), visible in backscatter; and D)
572 three K-feldspar grains (each with visible overgrowths), with laser ablation pits shown on the
573 largest grain.
574
575 **Figure 4:** $^{206}Pb/^{204}Pb$ vs. $^{207}Pb/^{204}Pb$ plots showing A) K-feldspar data from the East Irish Sea
576 Basin (EISB) Ormskirk Sandstone Formation sandstones; B) K-feldspar data from the Wessex
577 Basin (WB) Otter Sandstone Formation; C) the enclosed range of Pb isotopic composition of all
578 K-feldspar grains from EISB and WB sandstones, illustrating clear overlap between the two and
579 suggesting that the sandstones from each basin have the same provenance; and D) the Pb
580 isotopic composition of all K-feldspar grains analysed from EISB fluvial facies, EISB aeolian
581 facies and WB fluvial facies sandstones, indicating that there are no significant differences in the
582 Pb composition of K-feldspar grains from either facies. 'Far.' indicates grains analysed using
583 Faraday collector configuration, 'IC' indicates ion counter collector configuration used. When not
584 indicated, the IC configuration was used.
585
586 **Figure 5:** $^{206}Pb/^{204}Pb$ vs. $^{207}Pb/^{204}Pb$ plots of EISB and WB K-feldspars against A) new data from
587 Variscan granites (Brittany, Normandy and Cornwall), Cadomian Granite and a single clast of
588 feldspar porphyry from the Budleigh Salterton Pebble Beds (BSPB) ; B) published data from
589 Variscan Granites from Brittany, Cornwall, the French Massif Central and the Pyrennes; C) new

and published data from Irish Massif granites, granitic veins (cutting the Rosslare Complex) and galena; D) published data from Scottish granites and granitic rocks and granites from northern England; E) summary of potential groupings and suggested sources for the feldspars. Pb basement data from Blaxland *et al.* 1979; Vitrac *et al* .1981; Kinnaird e*t al.* 2002; Tyrrell *et al.* 2006. New basement data are shown in Table 2.

Figure 6: $^{206}Pb/^{204}Pb$ vs. $^{207}Pb/^{204}Pb$ plot showing the Pb isotopic composition of all K-feldspar grains analysed from the East Irish Sea (EISB) and Wessex (WB) basin Triassic sandstones. Also shown is the range of compositions found in detrital K-feldspars Permo-Triassic and Triassic sandstones in basins more marginal to NW Europe, from Upper Carboniferous sandstones in the Pennine Basin (Data from Tyrrell *et al.* 2006, 2007, 2009, 2010) and Lower Carboniferous sandstones in the Irish NW Carboniferous Basin (Data in table 2).

Figure 7: Schematic palaeogeographic reconstruction of the Middle Triassic (after Scotese 2002; Eide 2002; McKie & Williams 2009; Bourquin *et al* .2011; McKie & Shannon 2011) showing the distribution of massifs and sedimentary basins, with potential K-feldspar sources highlighted. Also highlighted are potential drainage directions and sedimentary input points for the 'Budleighensis' system, as suggested by the data presented in this paper, and for the Triassic basins more marginal to NW Europe (after Tyrrell *et al.* 2010). Abbreviations are listed in caption figure 1. The approximate palaeogeographic location of Pb basement data in Figure 4 is shown; B&C = Brittany and Cornwall granites; BfG = Barfleur Granite; BrG = Brech Granite; CG = Carnsore Granite; ClG = Carrolles Granite; FlG = Flamanville Granite, FMC = French Massif Central granites; LEG = Land's End Granite; LnG = Leinster Granite; MmS =Mullaghmore Sandstone Formation. PY = Pyrennes Granites; ShG = Shap Granite; SIga = southern Ireland Galena data; SUG = Southern Uplands granites; RC = Rosslare Complex.

Figure 8: Schematic block diagram showing the distribution of uplands in the Middle Triassic, with suggested drainage routes and sediment storage areas highlighted. The block diagram shows that there is major topography within the remnant Variscan Uplands and perhaps within the Greenland Massif, but that the topography of the Scottish and Irish Massifs is relatively subdued. The Scottish and Irish massifs act as a drainage divide separating systems influenced by the Variscan Uplands from those with no Variscan input.

References:

627 Alizai, A., Clift, P.D. Giosan, L., VanLaningham, S., Hinton, R., Tabrez, A. R., Danish, M. & the
628 Edinburgh Ion Microprobe Facility (EIMF). 2011. Pb isotopic variability in the modern-Pleistocene
629 Indus River system measured by ion microprobe in detrital K-feldspar grains. *Geochimica et*
630 *Cosmochimica Acta,* 75, 4771-4795. doi:10.1016/j.gca.2011.05.039
631
632 Allen P., Bennett S.D., Cunningham, M.J.M., Carter, A., Gallagher, K., Laz-Zaretti, E., Galewsky,
633 J., Densmore, A.L., Phillips, W.E.A., Naylor, D. & Hach, C.S. 2002. The Post-Variscan Thermal
634 and Denudational History of Ireland. In: Doré, A.G., Cartwright, J.A., Stoker, M.S., Turner, J.P.
635 and White, N. (eds) *Exhumation of the North Atlantic Margin: Timing, Mechanism and*
636 *Implications for Petroleum Exploration.* Geological Society London, Special Publications, 196,
637 371-399. doi: 10.1144/GSL.SP.2002.196.01.20
638
639 Audley-Charles, M.G. 1970. Triassic palaeogeography of the British Isles. *Quarterly Journal of*
640 *the Geological Society, London,* 126, 49-89. doi: 10.1144/gsjgs.126.1.0049
641
642 Blaxland, A.B., Aftalion, M. & Van Breemen, O. 1979. Pb isotopic composition of feldspars from
643 Scottish Caledonian Granites, and the nature of the underlying crust. *Scottish Journal of Geology*,
644 15, 139-151. doi: 10.1144/sjg15020139
645
646 Bourquin, S., Guillocheau, F. & Péron, S. 2009. Braided rivers within an arid alluvial plain
647 (example from the Lower Triassic, western German Basin): recognition criteria and expression of
648 stratigraphic cycles. *Sedimentology*, 56, 2235–2264. doi: 10.1111/j.1365-3091.2009.01078.x
649
650 Bourquin, S., Bercovici, A., López-Gómez, J., Diez, J. B., Broutin, J., Ronchi, A., Durand, M.,
651 Arché, A., Linol, B. & Amour, F. 2011. The Permian–Triassic transition and the onset of Mesozoic
652 sedimentation at the northwestern peri-Tethyan domain scale: Palaeogeographic maps and
653 geodynamic implications. *Palaeogeography, Palaeoclimatology, Palaeoecology*, 299, 265-280.
654 doi: 10.1016/j.palaeo.2010.11.007
655
656 Brookfield, M.E. 2004. The enigma of fine-grained alluvial basin fills: the Permo-Triassic
657 (Cumbrian Coastal and Sherwood Sandstones Groups) of the Solway Basin, NW England and
658 SW Scotland). *International Journal of Earth Sciences (Geologische Rundschau)*, 93, 282–296.
659 doi: 10.1007/s00531-004-0381-z
660
661 Clift, P.D., Van Long, H., Hinton, R., Ellam, R.M., Hannigan, R., Tan, M.T., Blusztajn, J. & Duc,
662 N.A. 2008. Evolving east Asian river systems reconstructed by trace element and Pb and Nd

663 isotope variations in modern and ancient Red River-Song Hong sediments. *Geochemistry*
664 *Geophysics Geosystems,* 9, Q04039. doi:10.1029/2007GC001867
665
666 Dancer, P.N., Kenyon-Roberts, S.M., Downey, J.W., Baillie, J.M., Meadows, N.S. & Maguire, K.
667 2005. The Corrib gas field, offshore west of Ireland. *In*: Doré, A.G. & Vining, B.A. (eds.)
668 *Petroleum Geology: North-West Europe and Global Perspectives – Proceedings to the 6th*
669 *Petroleum Geology Conference.* Geological Society, London, 1035-1046. doi: 10.1144/0061035
670
671 Eide, E.A. 2002. *BATLAS – Mid Norway plate reconstruction atlas with global and North Atlantic*
672 *perspectives*. Geological Survey of Norway.
673
674 Gibbons, W. and Horak, J.M., 1996. Evolution of the Neoproterozoic Avalonian subduction
675 system: Evidence from the British Isles, Avalonian and related Peri-Gondwanan terranes of the
676 circum-North Atlantic. *Geological Society of America Special Paper*, 304, 269-280.
677
678 Hall, A. & Bishop, P. 2002. Scotland's denudational history: an integrated view of erosion and
679 sedimentation at an uplifted passive margin. In: Doré, A.G., Cartwright, J.A., Stoker, M.S.,
680 Turner., J.P. and White, N. (eds) *Exhumation of the North Atlantic Margin: Timing, Mechanisms*
681 *and Implications for Petroleum Exploration*. Geological Society Special Publication, 196, 271-290.
682 doi:10.1144/GSL.SP.2002.196.01.15
683
684 Hounslow, M.W. & McIntosh, G. 2003. Magnetostratigraphy of the Sherwood Sandstone Group
685 (Lower and Middle Triassic), south Devon, UK: detailed correlation of the marine and non-marine
686 Anisian. *Palaeogeography, Palaeoclimatology, Palaeoecology,* 193, 325-348. doi:
687 10.1016/S0031-0182(03)00235-9
688
689 Hounslow, M.W. & Ruffell, A.H. 2006. Triassic: seasonal rivers, dusty deserts and saline lakes.
690 In: Brenchley, P.J. & Rawson, P.F. (eds) *Geology of England and Wales*, Geological Society of
691 London, 295-324.
692
693 Kinnaird, J.A., Ixer R.A., Barriero, B. & Nex, P.A.M. 2002. Contrasting sources for lead in Cu-
694 polymetallic and Zn-Pb mineralisation in Ireland: constraints from lead isotopes. *Mineralium*
695 *Deposita*, 37, 495-511. doi: 10.1007/s00126-001-0252-5
696
697 Knudsen, T-L. 2001. Contrasting provenance of Triassic/Jurassic sediments in North
698 Sea Rift: a single zircon (SIMS), Sm–Nd and trace element study. *Chemical Geology,* 171, 273–
699 293. doi: 10.1016/S0009-2541(00)00253-9

Koppen, A. & Carter, A. 2000. Constraints on provenance of the central European Triassic using detrital zircon fission track data. *Palaeogeography, Palaeoclimatology, Palaeoecology*, 161, 193–204. doi: 10.1016/S0031-0182(00)00123-1

Kutzbach, J.E. & Gallimore, R.G. 1989. Pangean climates: megamonsoons of the megacontinent. *Journal of Geophysical Research,* 94, 3341-3357. doi: 10.1029/JD094iD03p03341

Le Maitre, R.W. 2002. *Igneous Rocks: A Classification and Glossary of Terms*, Cambridge University Press.

Lewis, C.L.E., Green, P.F., Carter, R, A., Hurford, A.J. 1992. Elevated K/T palaeotemperatures throughout Northwest England: three kilometres of Tertiary erosion? *Earth and Planetary Science Letters*, 112, 131-145. doi: 10.1016/0012-821X(92)90012-K

Mange-Rajetzky, M. 1995. Subdivision and correlation of monotonous sandstone sequences using high-resolution heavy mineral analysis, a case study: the Triassic of the Central Graben. In: Dunay, R.E., Hailwood, E.A. (eds) *Non-biostratigraphical Methods of Dating and Correlation*, Geological Society of London, Special Publication, 89, 23-30. doi: 10.1144/ GSL.SP.1995.089.01.03

Mange, M., Turner, P., Ince, D., Pugh, J. & Wright, D. 1999. A new perspective on the zonation and correlation of barren strata: an integrated heavy mineral and palaeomagnetic study of the Sherwood Sandstone Group, East Irish Sea Basin and surrounding areas. *Journal of Petroleum Geology*, 22, 325-348. doi: 10.1111/j.1747-5457.1999.tb00990.x

McKie, T., Aggett, J. & Hogg, A.J.C. 1997. Sequence architecture of a Triassic semi-arid, fluvio-lacustrine reservoir, Wytch Farm Field, southern England. In: Shanley K.W., Perkins, B.F. (eds) *Shallow marine and nonmarine reservoirs: sequence stratigraphy, reservoir architecture and production characteristics*, 18th Annual SEPM Gulf Coast Section Research Conference Proceedings, 197-207.

McKie, T., Aggett, J. & Hogg, A.J.C. 1998. Reservoir architecture of the upper Sherwood Sandstone, Wytch Farm Field, southern England. In: Underhill, J.R. (ed) *The development and evolution of the Wessex Basin and adjacent areas*. Geological Society of London, Special Publication, 133, 399-406. doi: 10.1144/GSL.SP.1998.133.01.21

McKie, T. & Williams, B.P. 2009. Triassic palaeogeography and fluvial dispersal across the northwest European Basins. *Geological Journal,* 44, 711–741. doi: 10.1002/gj.1201

McKie, T. & Shannon, P.M. 2011. Comment on "The Permian–Triassic transition and the onset of Mesozoic sedimentation at the northwestern peri-Tethyan domain scale: Palaeogeographic maps and geodynamic implications" by Bourquin, S., Bercovici, A., López-Gómez, J., Diez, J.B., Broutin, J., Ronchi, A., Durand, M., Arché, A., Linol B. & Amour, F. *Palaeogeography, Palaeoclimatology, Palaeoecology*, 311, 136-143. doi:10.1016/j.palaeo.2011.07.016

Meadows, N.S. & Beach, A. 1993. Structural and climatic controls on facies distribution in a mixed fluvial and aeolian reservoir; the Triassic Sherwood Sandstone in the Irish Sea. In: North, C.P. (ed) *Characterization of fluvial and aeolian reservoirs.* Geological Society of London, Special Publications, 73, 247-264. doi: 10.1144/GSL.SP.1993.073.01.15

Meadows, N.S. 2004. The sedimentology and stratigraphy of the early Triassic Sherwood Sandstone Group in the East Irish Sea and Cheshire basins of NW England. *Unpublished PhD Thesis,* Trinity College Dublin.

Meadows, N.S. 2006. The correlation and sequence architecture of the Ormskirk Sandstone Formation in the Triassic Sherwood Sandstone Group of the East Irish Sea Basin, NW England. *Geological Journal*, **41**, 93-122. doi: 10.1002/gj.1034.

Mearns, E.W., Knarud, R., Raestad, N., Stanley, K.O. & Stockbridge CP. 1989. Samarium-neodymium isotope stratigraphy of the Lunde and Statfjord formations of Snorre oil field, northern North Sea. *Journal of the Geological Society, London*, 146, 217-228. doi: 10.1144/ gsjgs.146.2.0217

Mountney, N.P. and Thompson, D.B. 2002. Stratigraphic evolution and preservation of aeolian dune and damp/wet interdune strata: an example from the Triassic Helsby Sandstone Formation, Cheshire Basin, UK. *Sedimentology*, 49, 805-833. doi: 10.1046/j.1365-3091.2002.00472.x

Naylor, D. and Shannon, P.M. 2011. The Petroleum Geology of Ireland. Dunedin Academic Press. 262pp

Praeg, D. 2004. Diachronous Variscan late-orogenic collapse as a response to multiple detachments: a view from the internides in France to the foreland in the Irish Sea. *In:* Wilson, M.,

774 Neumann, E.-R., Davies, G.R., Timmerman, M.J., Heeremans, M. & Larsen, B.T. (eds) *Permo-*
775 *Carboniferous Magmatism and Rifting in Europe.* Geological Society, London, Special
776 Publications, 223, 89-138. doi: 10.1144/GSL.SP.2004.223.01.05
777
778 Preston, J., Hartley, A., Hole, M., May, G., Mange-Rajetzky, M., Buck, S. & Vaughan, L. 2002.
779 The provenance of Triassic continental sandstones from the Beryl Field, northern North Sea:
780 mineralogical, geochemical, and sedimentological constraints. *Journal of Sedimentary Research*,
781 72, 18-29. doi: 10.1306/042201720018
782
783 Preto, N. Kustatscherc, E. & Wignall, P.B., 2010. Triassic climates — State of the art and
784 perspectives. *Palaeogeography, Palaeoclimatology, Palaeoecology*, 290, 1-10. doi:
785 10.1016/j.palaeo.2010.03.015
786
787 Redfern, J., Shannon, P.M., Tyrrell, S., Leleu, S., Fabuel Perez, I., Baudon, C., Haughton,
788 P.D.W., Daly, J.S., Van Lanen, X., Štolfová, K., Hodgetts, D., Williams, B. & Speksnijder, A.,
789 2010. An integrated study of Permo -Triassic basins along the North Atlantic passive margin:
790 implication for future exploration. In: Vining, B. & Pickering S.C. (eds.); *From Mature Basins to*
791 *New Frontiers: Proceedings of the 7th Petroleum Geology Conference*. Geological Society of
792 London, 921-936. doi: 10.1144/0070921
793
794 Ruffell, A. & Shelton, R. 1999. The control of sedimentary facies by climate during phases of
795 crustal extension; examples from the Triassic of onshore and offshore England and Northern
796 Ireland. *Journal of the Geological Society, London*, 156, 779-789. doi: 10.1144/gsjgs.156.4.0779
797
798 Scotese, C.R. 2002. http://www.scotese.com (PALEOMAP website).
799
800 Smith, S.A. 1990. The sedimentology and accretionary styles of an ancient gravel-bed stream:
801 the Budleigh Salterton Pebble Beds (Lower Triassic), southwest England. *Sedimentary Geology,*
802 67, 199-219. doi:10.1016/0037-0738(90)90035-R
803
804 Smith, S.A. & Edwards, R.A. 1991. Regional sedimentological variations in Lower Triassic fluvial
805 conglomerates (Budleigh Salterton Pebble Beds), southwest England: some implications for
806 palaeogeography and basin evolution. *Geological Journal*, **26**, 65-83. doi:
807 10.1002/gj.3350260105
808
809

Štolfová, K. & Shannon, P.M. 2009. Permo-Triassic development from Ireland to Norway: Basin architecture and regional controls. *Geological Journal,* 44*,* 692-710. doi: 10.1002/gj.1187

Szulc, J. 1999. Anisian-Carnian evolution of the Germanic basin and its eustatic, tectonic and climatic controls. In: Bachmann, G.H. & Lerche, I. (eds.): *Epicontinental Triassic.* Zentralblatt für Geologie und Paläeontologie, 7-8, 813–852, Stuttgart.

Tyrrell. S., Haughton, P.D.W., Daly, J.S., Kokfelt, T.F. & Gagnevin, D. 2006. The use of the common Pb isotope composition of detrital K-feldspar grains as a provenance tool and its application to Upper Carboniferous palaeodrainage, Northern England. *Journal of Sedimentary Research,* 76, 324-345. doi: 10.2110/jsr.2006.023

Tyrrell, S., Haughton, P.D.W. & Daly, J.S. 2007. Drainage re-organization during break-up of Pangea revealed by *in-situ* Pb isotopic analysis of detrital K-feldspar. *Geology,* 35, 971-974. doi: 10.1130/G4123A

Tyrrell, S., Leleu, S., Souders, A.K., Haughton, P.D.W. & Daly, J.S. 2009. K-feldspar sand-grain provenance in the Triassic, west of Shetland: a first-cycle sedimentary fingerprint? *Geological Journal,* 44*,* 692-710. doi: 10.1002/gj.1185

Tyrrell, S., Souders, A.K., Haughton, P.D.W., Daly, J.S. & Shannon, P.M. 2010. Sandstone provenance and palaeodrainage on the eastern Rockall Basin margin: evidence from the Pb isotopic composition of detrital K-feldspar. In: Vining, B. & Pickering, S.C., (eds.); *From Mature Basins to New Frontiers: Proceedings of the 7th Petroleum Geology Conference*. Geological Society of London, 937-952. doi:10.1144/0070937

Vitrac, A.M., Albarède, F. & Allégre, C.J., 1981. Lead isotopic composition of Hercynian granite K-feldspars constrains continental genesis. *Nature*, 291, 460-464. doi:10.1038/291460a0

Warrington, G., Audley-Charles, M.G., Elliot, R.E., Evans, W.B., Ivimey-Cook, H.C., Kent, P.E., Robinson, P.L., Shotton, F.W. & Taylor, F.M. 1980. A correlation of Triassic rocks in the British Isles. *Special Reports of the Geological Society of London,* 13.

Warrington, G. & Ivimey-Cooke, H.C. 1992. Triassic. *In:* Cope, J.C.W., Ingham, J.K. & Rawson, P.F. (eds.) *Atlas of Palaeogeography and Lithofacies.* Geological Society, London, Memoir, **13,** 97-106.

Wills, L.J., 1970. The Triassic succession in the central Midlands in its regional setting. *Quarterly Journal of the Geological Society, London,* 126, 225-283. doi: 10.1144/gsjgs.126.1.0225

Wills, W., 1950. *The palaeogeography of the Midlands*, University Press, Liverpool.

Ziegler, P.A. 1992. *Geological Atlas of Western and Central Europe*. Geological Society Publishing House. Shell International Petroleum Maatschappij B.V.

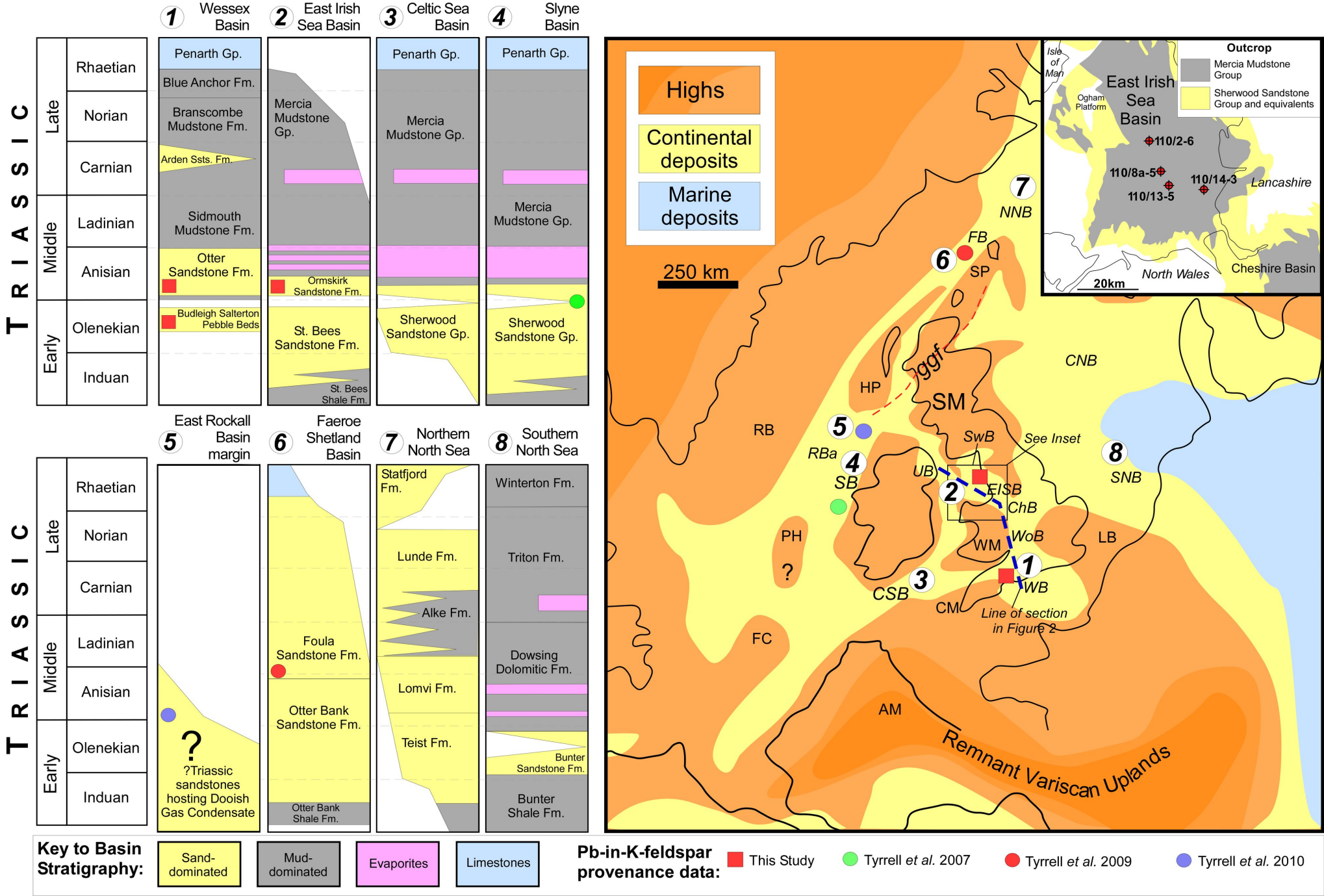
TRIASSIC
Late
Middle
Early
Rhaetian
Norian
Carnian
Ladinian
Anisian
Olenekian
Induan
1 Wessex Basin
Penarth Gp.
Blue Anchor Fm.
Branscombe Mudstone Fm.
Arden Ssts. Fm.
Sidmouth Mudstone Fm.
Otter Sandstone Fm.
Budleigh Salterton Pebble Beds
2 East Irish Sea Basin
Penarth Gp.
Mercia Mudstone Gp.
Ormskirk Sandstone Fm.
St. Bees Sandstone Fm.
St. Bees Shale Fm.
3 Celtic Sea Basin
Penarth Gp.
Mercia Mudstone Gp.
Sherwood Sandstone Gp.
4 Slyne Basin
Penarth Gp.
Mercia Mudstone Gp.
Sherwood Sandstone Gp.
5 East Rockall Basin margin
?
?Triassic sandstones hosting Dooish Gas Condensate
6 Faeroe Shetland Basin
Foula Sandstone Fm.
Otter Bank Sandstone Fm.
Otter Bank Shale Fm.
7 Northern North Sea
Statfjord Fm.
Lunde Fm.
Alke Fm.
Lomvi Fm.
Teist Fm.
8 Southern North Sea
Winterton Fm.
Triton Fm.
Dowsing Dolomitic Fm.
Bunter Sandstone Fm.
Bunter Shale Fm.
Highs
Continental deposits
Marine deposits
250 km
NNB
CNB
SNB
FB
SP
ggf
HP
SM
RB
RBa
SB
UB
SwB
See Inset
EISB
ChB
WoB
WB
WM
LB
PH
?
CSB
CM
FC
AM
Remnant Variscan Uplands
Line of section in Figure 2
Isle of Man
Ogham Platform
East Irish Sea Basin
110/2-6
110/8a-5
110/13-5
110/14-3
Lancashire
North Wales
Cheshire Basin
20km
Outcrop
Mercia Mudstone Group
Sherwood Sandstone Group and equivalents
Key to Basin Stratigraphy:
Sand-dominated
Mud-dominated
Evaporites
Limestones
Pb-in-K-feldspar provenance data:
This Study
Tyrrell et al. 2007
Tyrrell et al. 2009
Tyrrell et al. 2010

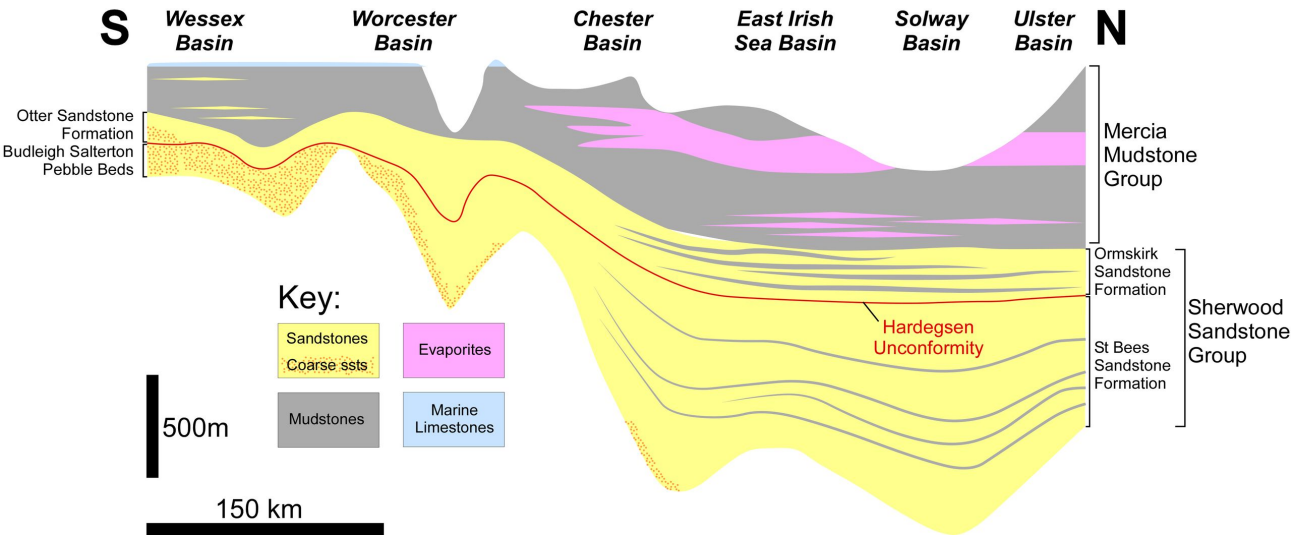
S
Wessex Basin
Worcester Basin
Chester Basin
East Irish Sea Basin
Solway Basin
Ulster Basin
N
Otter Sandstone Formation
Budleigh Salterton Pebble Beds
Mercia Mudstone Group
Ormskirk Sandstone Formation
Sherwood Sandstone Group
St Bees Sandstone Formation
Hardegsen Unconformity
Key:
Sandstones Coarse ssts
Evaporites
Mudstones
Marine Limestones
500m
150 km

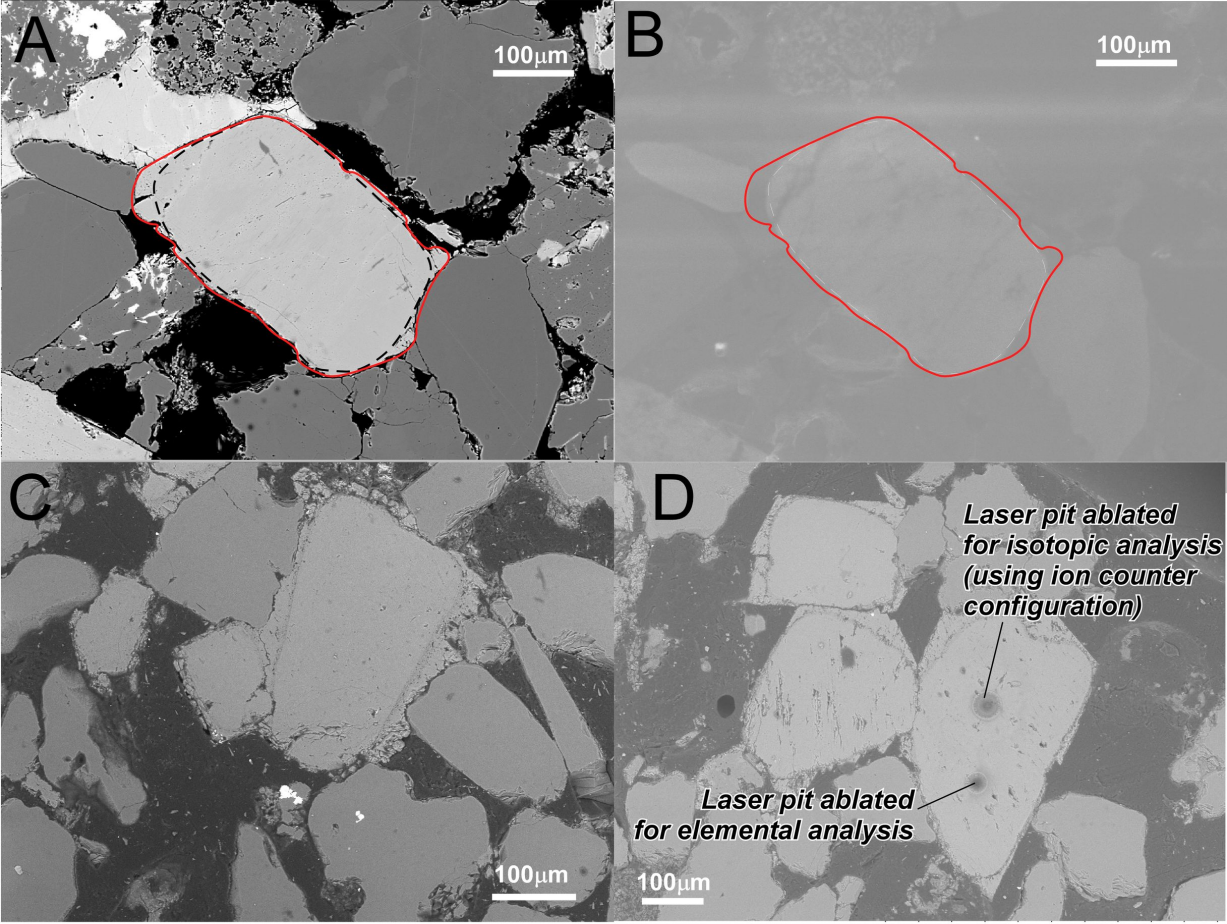
A
100μm
B
100μm
C
100μm
D
Laser pit ablated for isotopic analysis (using ion counter configuration)
Laser pit ablated for elemental analysis
100μm

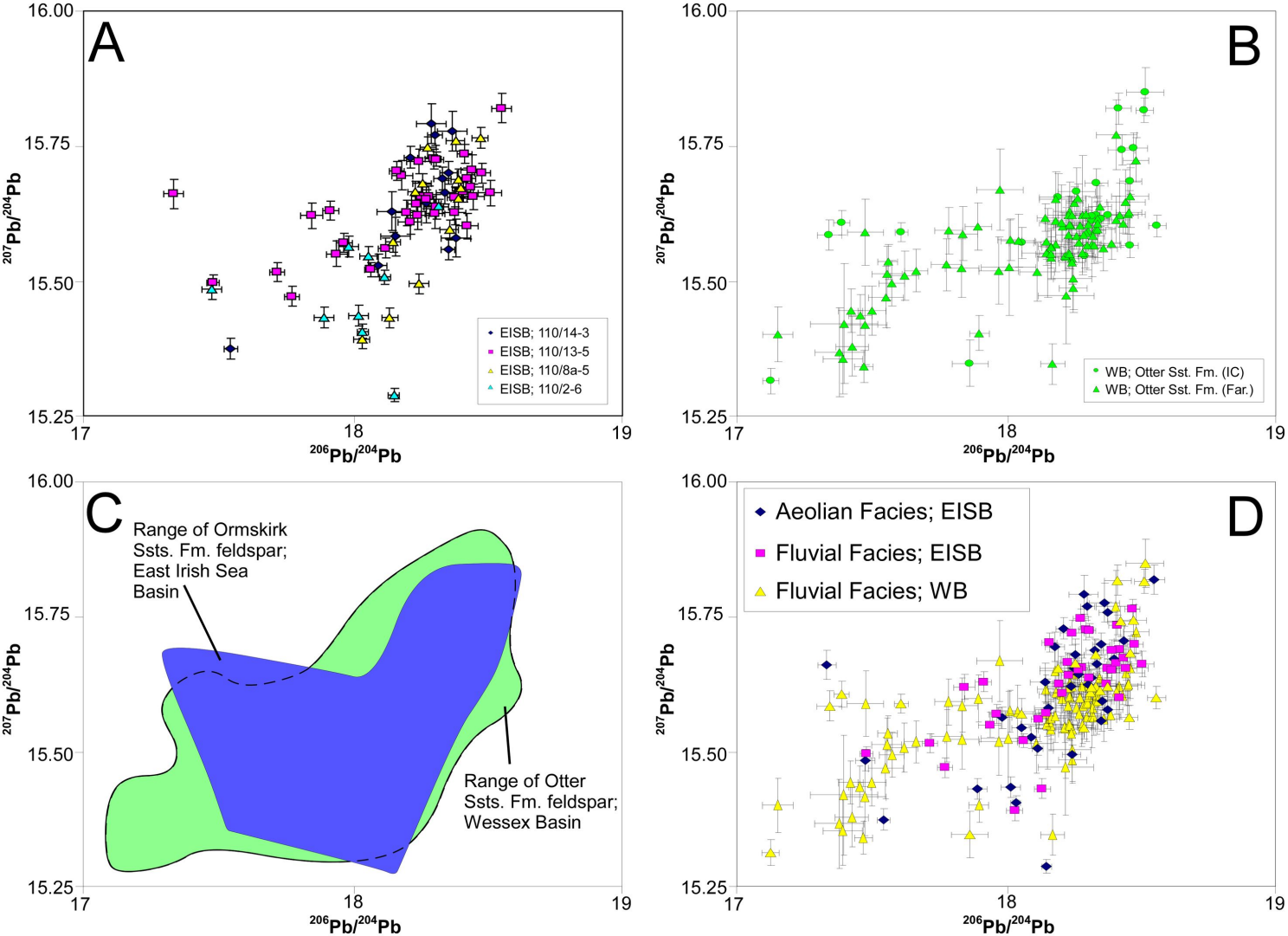
A
16.00
15.75
15.50
15.25
17
18
19
$^{207}Pb/^{204}Pb$
$^{206}Pb/^{204}Pb$
EISB; 110/14-3
EISB; 110/13-5
EISB; 110/8a-5
EISB; 110/2-6
B
WB; Otter Sst. Fm. (IC)
WB; Otter Sst. Fm. (Far.)
C
Range of Ormskirk Ssts. Fm. feldspar; East Irish Sea Basin
Range of Otter Ssts. Fm. feldspar; Wessex Basin
D
Aeolian Facies; EISB
Fluvial Facies; EISB
Fluvial Facies; WB

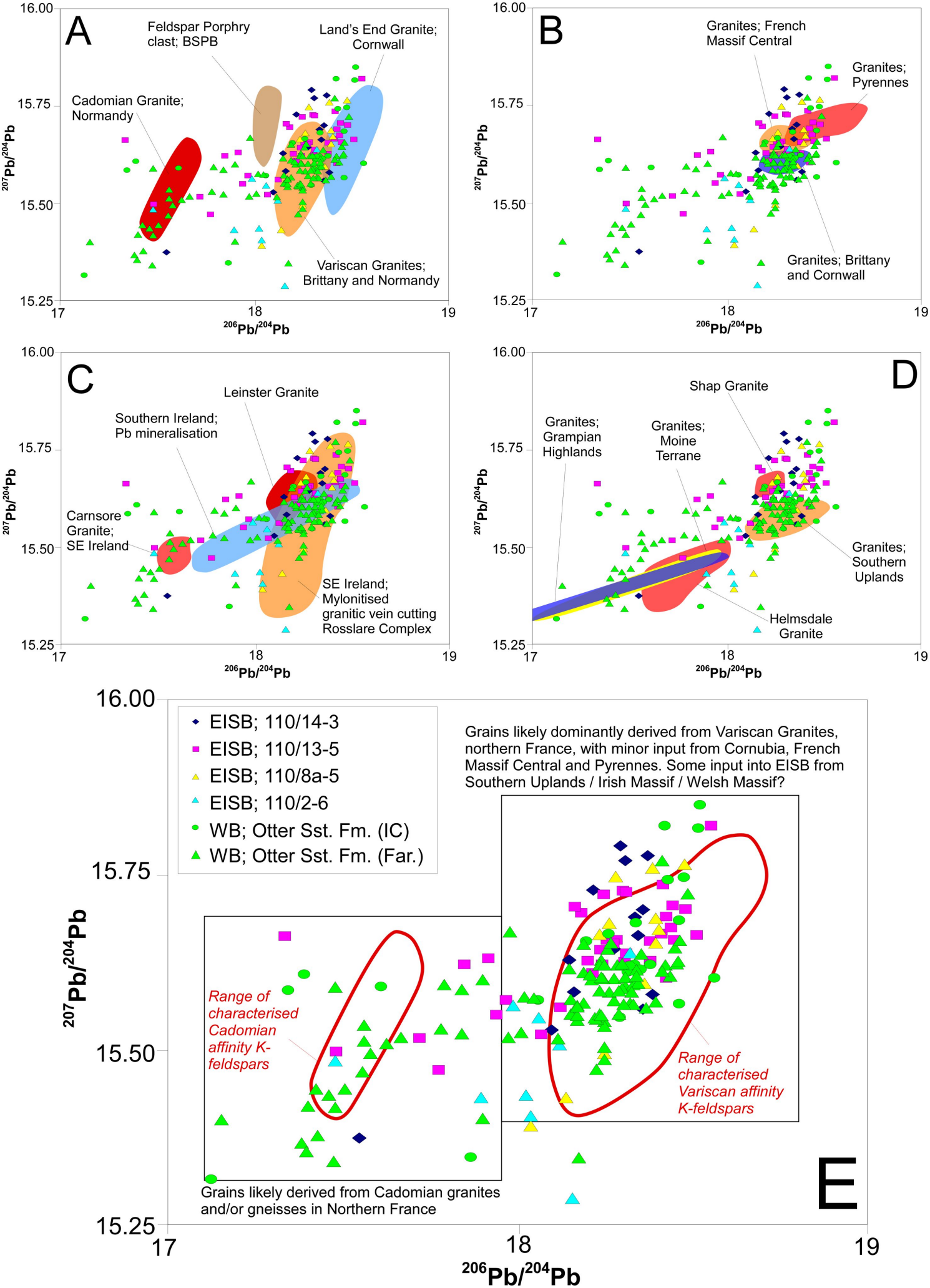
A
Feldspar Porphry clast; BSPB
Land's End Granite; Cornwall
Cadomian Granite; Normandy
Variscan Granites; Brittany and Normandy
B
Granites; French Massif Central
Granites; Pyrennes
Granites; Brittany and Cornwall
C
Leinster Granite
Southern Ireland; Pb mineralisation
Carnsore Granite; SE Ireland
SE Ireland; Mylonitised granitic vein cutting Rosslare Complex
D
Shap Granite
Granites; Grampian Highlands
Granites; Moine Terrane
Granites; Southern Uplands
Helmsdale Granite
E
EISB; 110/14-3
EISB; 110/13-5
EISB; 110/8a-5
EISB; 110/2-6
WB; Otter Sst. Fm. (IC)
WB; Otter Sst. Fm. (Far.)
Grains likely dominantly derived from Variscan Granites, northern France, with minor input from Cornubia, French Massif Central and Pyrennes. Some input into EISB from Southern Uplands / Irish Massif / Welsh Massif?
Range of characterised Cadomian affinity K-feldspars
Range of characterised Variscan affinity K-feldspars
Grains likely derived from Cadomian granites and/or gneisses in Northern France
16.00
15.75
15.50
15.25
17
18
19
207Pb/204Pb
206Pb/204Pb

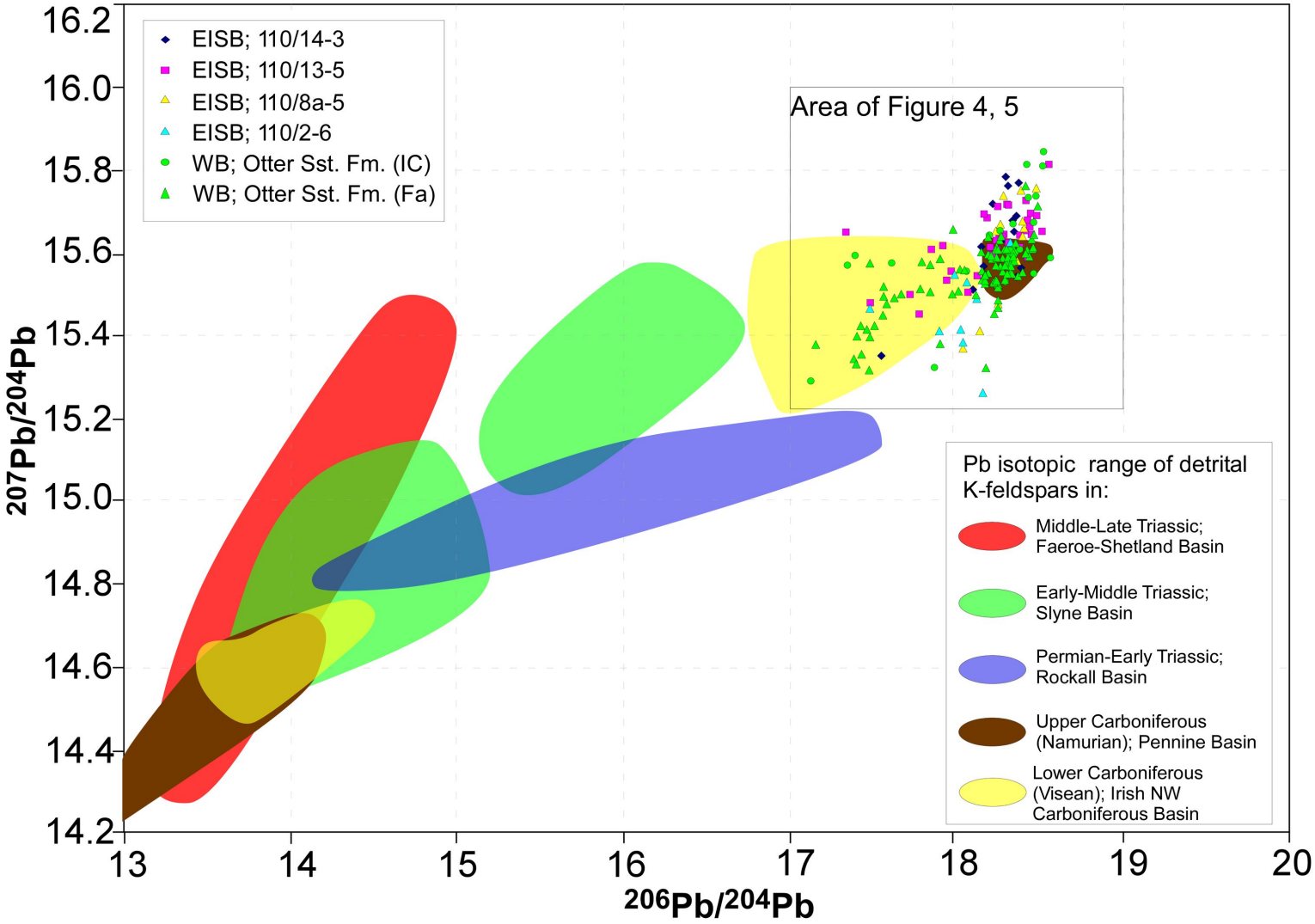
EISB; 110/14-3
EISB; 110/13-5
EISB; 110/8a-5
EISB; 110/2-6
WB; Otter Sst. Fm. (IC)
WB; Otter Sst. Fm. (Fa)
Area of Figure 4, 5
Pb isotopic range of detrital K-feldspars in:
Middle-Late Triassic; Faeroe-Shetland Basin
Early-Middle Triassic; Slyne Basin
Permian-Early Triassic; Rockall Basin
Upper Carboniferous (Namurian); Pennine Basin
Lower Carboniferous (Visean); Irish NW Carboniferous Basin
16.2
16.0
15.8
15.6
15.4
15.2
15.0
14.8
14.6
14.4
14.2
207Pb/204Pb
13
14
15
16
17
18
19
20
206Pb/204Pb

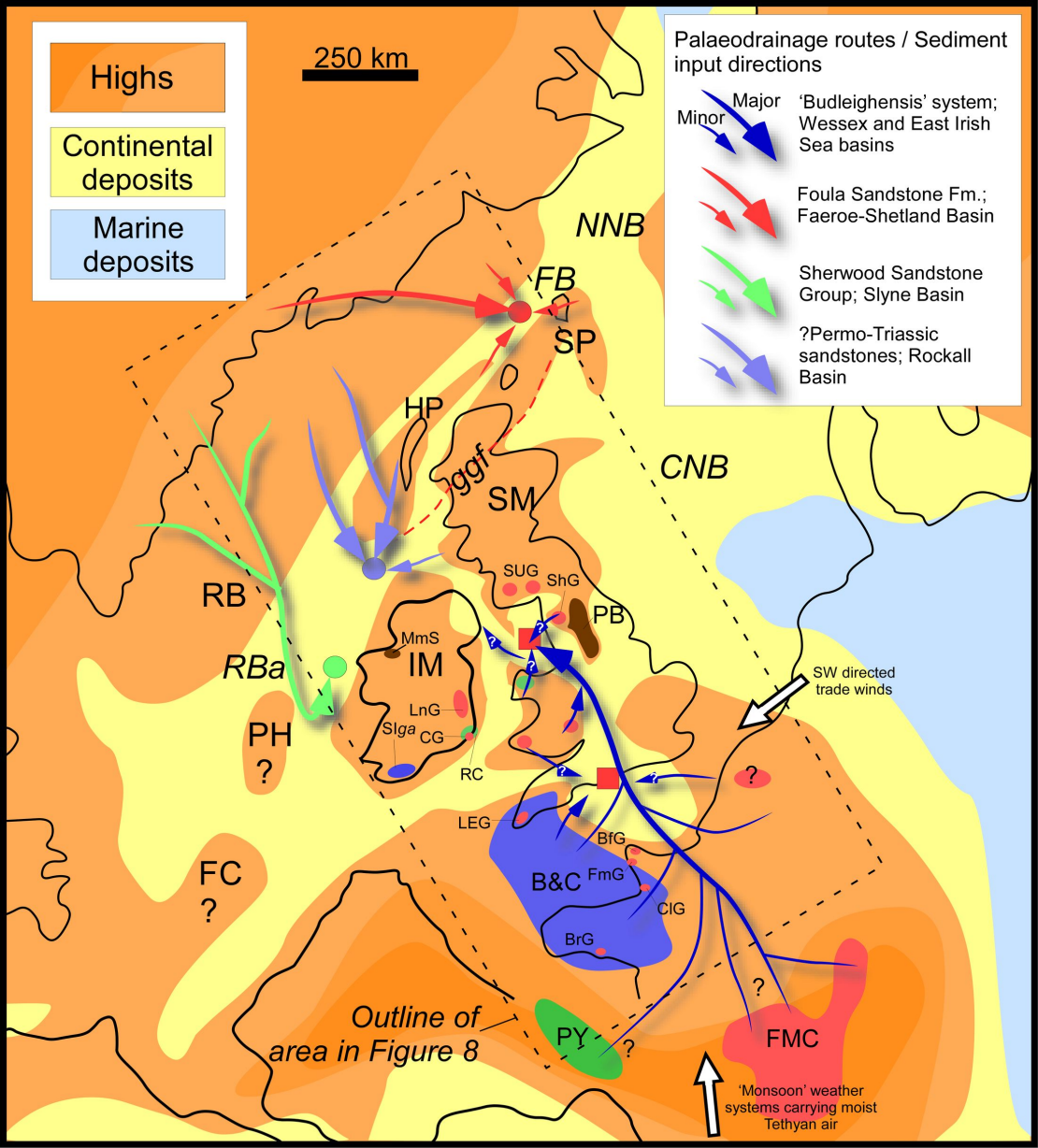
Highs
Continental deposits
Marine deposits
250 km
Palaeodrainage routes / Sediment input directions
Major
Minor
'Budleighensis' system; Wessex and East Irish Sea basins
Foula Sandstone Fm.; Faeroe-Shetland Basin
Sherwood Sandstone Group; Slyne Basin
?Permo-Triassic sandstones; Rockall Basin
NNB
FB
SP
HP
ggf
CNB
SM
RB
RBa
PH
?
IM
MmS
LnG
Slga
CG
RC
SUG
ShG
PB
SW directed trade winds
LEG
BfG
B&C
FmG
ClG
BrG
FC
?
Outline of area in Figure 8
PY
FMC
'Monsoon' weather systems carrying moist Tethyan air

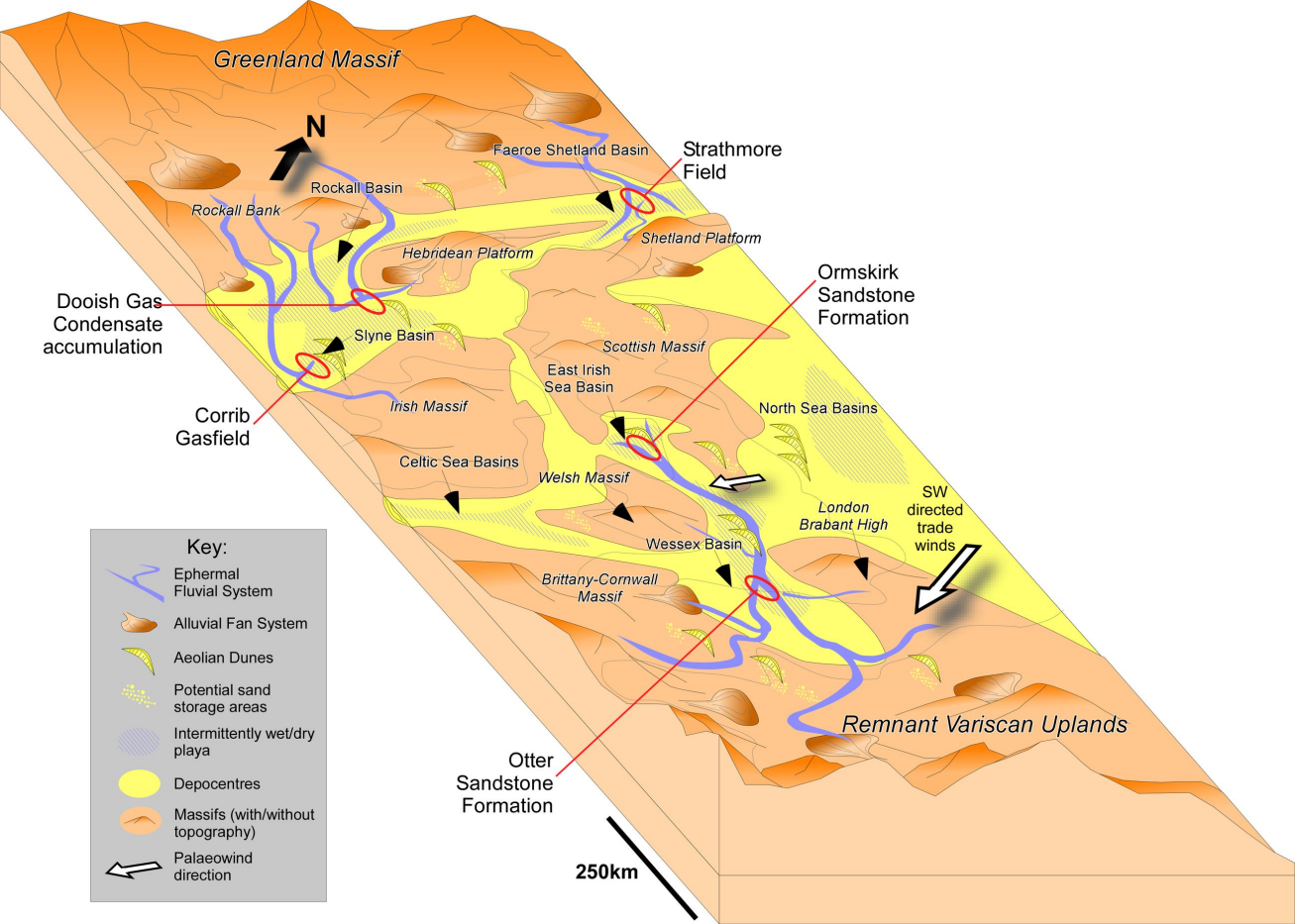
Greenland Massif
N
Faeroe Shetland Basin
Strathmore Field
Rockall Basin
Rockall Bank
Shetland Platform
Hebridean Platform
Ormskirk Sandstone Formation
Dooish Gas Condensate accumulation
Slyne Basin
Scottish Massif
East Irish Sea Basin
Corrib Gasfield
Irish Massif
North Sea Basins
Celtic Sea Basins
Welsh Massif
SW directed trade winds
London Brabant High
Wessex Basin
Brittany-Cornwall Massif
Remnant Variscan Uplands
Otter Sandstone Formation
250km
Key:
Ephermal Fluvial System
Alluvial Fan System
Aeolian Dunes
Potential sand storage areas
Intermittently wet/dry playa
Depocentres
Massifs (with/without topography)
Palaeowind direction

Table 1: Pb, U and Th concentration and Pb isotopic data from feldspars from Triassic sandstones (and one clast) in the East Irish Sea (EISB) and Wessex (WB) basin. Also shown are the stratigraphic nomenclature, the age, depths, wells and facies interpretation of individual sandstone samples. EISB facies interpretations from Meadows, 2004.

Area; Well	Sample Ref.	Stratigraphy	Age	Facies	Depth (m)	Grain Ref.	Pb (ppm)	Th (ppm)	U (ppm)	$^{206}Pb/^{204}Pb$	2σ	$^{207}Pb/^{204}Pb$	2σ	$^{208}Pb/^{204}Pb$	2σ
East Irish Sea Basin; 110/14-3	2	Ormskirk Sandstone Fm.	Anisian	Aeolian sandsheet	1084.77	1	65.5	< 0.01	0.018	18.145	0.054	15.629	0.036	38.146	0.238
						2	11.5	< 0.01	0.015	18.271	0.055	15.644	0.036	38.087	0.241
						3	56.3	0.045	0.994	18.159	0.054	15.582	0.036	38.014	0.239
						5	50.6	< 0.01	< 0.01	18.380	0.055	15.579	0.036	38.128	0.240
						6	82.4	0.024	< 0.01	18.367	0.055	15.777	0.036	38.552	0.240
						8	72.1	< 0.01	< 0.01	18.290	0.055	15.782	0.036	38.492	0.241
	3	Ormskirk Sandstone Fm.	Anisian	Aeolian sandsheet	1085.85	1	81.7	0.047	0.176	18.095	0.031	15.528	0.021	37.847	0.205
						4	81.2	< 0.01	< 0.01	18.354	0.032	15.700	0.021	38.401	0.203
						5	14.6	0.148	0.038	18.341	0.032	15.664	0.022	38.246	0.210
						6	81.3	< 0.01	< 0.01	18.331	0.032	15.689	0.021	38.457	0.203
	4	Ormskirk Sandstone Fm.	Anisian	Aeolian sandsheet	1092.37	1	29.1	0.020	0.067	18.214	0.026	15.729	0.020	38.275	0.150
						2	5.02	0.012	0.036	18.353	0.026	15.598	0.020	37.822	0.148
						4	77.7	< 0.01	< 0.01	17.546	0.025	15.375	0.020	37.274	0.151
						5	156	0.059	0.017	18.304	0.029	15.721	0.020	38.420	0.149
East Irish Sea Basin; 110/13-5	7	Ormskirk Sandstone Fm.	Anisian	Aeolian sandsheet	885.6	1	71.2	0.030	0.044	18.242	0.037	15.622	0.027	38.158	0.173
						2	67.8	0.554	0.051	18.183	0.037	15.695	0.027	38.366	0.174
						3	68.2	< 0.01	0.012	18.256	0.037	15.696	0.027	38.322	0.172
						4	66	0.457	3.870	18.440	0.038	15.706	0.027	38.446	0.175
						5	124	0.021	0.085	18.551	0.038	15.820	0.027	38.629	0.179
						6	96.2	< 0.01	0.000	18.305	0.037	15.625	0.027	38.352	0.173
						7	46.3	1.670	0.041	17.334	0.036	15.661	0.027	37.592	0.173
	9	Ormskirk Sandstone Fm.	Anisian	Stacked fluvial channels	902.21	1	56	0.020	0.016	18.197	0.042	15.626	0.023	38.119	0.164
						3	45.7	0.113	0.347	18.375	0.042	15.627	0.023	38.345	0.165
						4	27	0.022	0.023	17.940	0.041	15.550	0.023	37.984	0.162
						5	143	< 0.01	< 0.01	18.422	0.042	15.602	0.023	38.293	0.164
						6	59.2	0.036	0.105	18.446	0.042	15.656	0.023	38.222	0.162
						7	79.2	< 0.01	< 0.01	17.845	0.041	15.621	0.023	38.071	0.164
						8	62.7	< 0.01	< 0.01	18.508	0.042	15.663	0.023	38.596	0.167
	10	Ormskirk Sandstone Fm.	Anisian	Stacked fluvial channels	904.95	1	88.8	0.032	0.022	17.718	0.028	15.516	0.018	38.052	0.100
						2	46.6	0.011	0.014	18.163	0.029	15.703	0.018	38.353	0.101
						3	68.1	0.016	< 0.01	18.378	0.029	15.655	0.018	38.394	0.103
						4	35.8	0.026	< 0.01	17.916	0.029	15.630	0.018	37.997	0.111
						5	138	0.854	0.462	18.281	0.029	15.657	0.018	38.403	0.100
						6	67.5	0.018	< 0.01	18.272	0.029	15.652	0.018	38.270	0.103
	11	Ormskirk Sandstone Fm.	Anisian	Stacked fluvial channels	916.2	7	11.3	0.041	0.001	17.968	0.029	15.570	0.018	38.218	0.100
						1	7.04	0.024	0.053	17.774	0.028	15.471	0.018	37.509	0.114
						2	75.8	0.014	< 0.01	18.234	0.028	15.642	0.018	38.404	0.113
						3	67.7	0.036	< 0.01	18.410	0.029	15.665	0.018	38.359	0.116
						4	54	< 0.01	< 0.01	18.480	0.029	15.700	0.018	38.419	0.115
						5	76.4	0.283	0.050	18.413	0.029	15.735	0.018	38.463	0.112
						6	132	0.021	0.053	18.425	0.029	15.690	0.018	38.356	0.116
						7	131	0.186	0.024	18.122	0.028	15.561	0.018	38.031	0.112
						8	96.5	< 0.01	< 0.01	18.298	0.029	15.726	0.018	38.351	0.116
	12	Ormskirk Sandstone Fm.	Anisian	Stacked fluvial channels	919.58	3	103	2.420	0.116	18.311	0.024	15.726	0.013	38.190	0.092
						5	66.9	< 0.01	0.013	17.481	0.023	15.497	0.013	37.458	0.089
						6	63	< 0.01	< 0.01	18.066	0.023	15.521	0.013	37.615	0.131
	16	Ormskirk Sandstone Fm.	Anisian	Stacked fluvial channels	960.73	1	40.1	0.027	0.032	18.311	0.046	15.638	0.022	38.158	0.171
						6	71.6	0.021	< 0.01	18.246	0.046	15.721	0.023	38.505	0.167
						7	161	0.136	0.187	18.211	0.045	15.608	0.022	38.101	0.164
						8	58.3	< 0.01	< 0.01	18.438	0.046	15.674	0.022	38.417	0.166
East Irish Sea Basin; 110/8a-5	20	Ormskirk Sandstone Fm.	Anisian	Aeolian sandsheet	1274.67	1	67.3	0.037	0.031	18.245	0.035	15.495	0.018	37.960	0.130
						2	78.6	0.012	0.112	18.257	0.034	15.681	0.019	38.470	0.130
						3	77.8	< 0.01	< 0.01	18.358	0.035	15.595	0.018	38.232	0.129
						4	171	< 0.01	0.026	18.380	0.035	15.759	0.019	38.397	0.132
						5	81.8	< 0.01	0.019	18.402	0.035	15.673	0.018	38.454	0.129
	21	Ormskirk Sandstone Fm.	Anisian	Stacked fluvial channels	1283.12	1	118	0.017	0.013	18.150	0.029	15.572	0.019	38.134	0.156
						2	169	< 0.01	0.011	18.032	0.029	15.392	0.018	37.675	0.156
						3	83.8	< 0.01	< 0.01	18.231	0.029	15.666	0.019	38.475	0.156
						4	55.4	0.258	0.035	18.472	0.029	15.765	0.019	38.734	0.158
						5	57.1	< 0.01	0.015	18.136	0.029	15.432	0.018	37.869	0.155
						7	138	< 0.01	< 0.01	18.393	0.029	15.652	0.019	38.681	0.158
						7	75.1	0.013	< 0.01	18.279	0.029	15.747	0.019	38.487	0.157
						8	94.8	< 0.01	< 0.01	18.394	0.029	15.688	0.019	38.393	0.158
East Irish Sea Basin; 110/2-6	25	Ormskirk Sandstone Fm.	Anisian	Aeolian sandsheet	955.33	1	200	0.048	< 0.01	17.985	0.036	15.564	0.020	38.148	0.146
						3	70.5	< 0.01	< 0.01	18.019	0.037	15.435	0.019	37.678	0.144
						5	48.8	< 0.01	< 0.01	17.892	0.036	15.432	0.019	37.439	0.146
						6	12.6	0.022	0.011	17.476	0.036	15.485	0.020	37.374	0.145
	28	Ormskirk Sandstone Fm.	Anisian	Aeolian dunes	965.61	1	97.1	< 0.01	< 0.01	18.119	0.019	15.507	0.013	38.034	0.091
						2	75.3	0.026	0.087	18.317	0.019	15.639	0.013	38.275	0.089
						3	30.2	0.536	< 0.01	18.152	0.019	15.289	0.013	37.416	0.097
						6	127	0.191	0.026	18.036	0.019	15.406	0.013	37.652	0.098
	39	Ormskirk Sandstone Fm.	Anisian	Damp sandflat	1116.48	1	76.9	0.071	0.165	18.056	0.033	15.546	0.017	37.959	0.099
Wessex Basin; Budleigh Salterton Outcrop	104	Otter Sandstone Fm.	Anisian			1	83.7	< 0.01	1.030	18.517	0.069	15.849	0.045	38.826	0.286
						2	81.8	0.073	0.046	18.194	0.069	15.655	0.044	38.448	0.291
						3	83	0.055	0.011	18.260	0.069	15.664	0.044	38.302	0.289
						4	85.1	< 0.01	< 0.01	17.896	0.067	15.347	0.043	37.559	0.272
						5	88.2	0.095	0.025	18.315	0.068	15.610	0.044	38.374	0.279
						F1*	na	na	na	18.146	0.030	15.617	0.026	38.225	0.064
						F2	na	na	na	18.149	0.026	15.551	0.022	37.966	0.055
						F3	na	na	na	17.575	0.047	15.495	0.041	37.546	0.102
						F4	na	na	na	18.114	0.064	15.516	0.055	37.894	0.135
						F5	na	na	na	18.285	0.040	15.551	0.034	38.093	0.084
						F6	na	na	na	18.325	0.041	15.566	0.035	38.152	0.085
						F7 (Repeat 3)	na	na	na	18.245	0.031	15.621	0.027	38.166	0.066
						F8	na	na	na	17.621	0.051	15.509	0.045	37.522	0.112
						F9	na	na	na	17.896	0.051	15.600	0.044	37.922	0.108
						F10	na	na	na	18.275	0.061	15.601	0.048	38.086	0.121
						F12	na	na	na	18.208	0.031	15.600	0.027	38.124	0.067
						F13	na	na	na	17.666	0.044	15.519	0.039	37.649	0.095
						F14	na	na	na	18.185	0.041	15.610	0.035	38.181	0.088
						F15	na	na	na	18.320	0.040	15.594	0.034	38.275	0.089
						F17	na	na	na	18.433	0.020	15.605	0.017	38.226	0.042
						F18	na	na	na	17.380	0.093	15.367	0.082	37.277	0.200
						F19	na	na	na	17.423	0.045	15.444	0.040	37.396	0.099
						F20	na	na	na	17.502	0.051	15.445	0.045	37.426	0.111
						F21	na	na	na	18.014	0.045	15.576	0.039	37.965	0.096
						F22	na	na	na	18.265	0.031	15.652	0.027	38.262	0.066
						F23	na	na	na	17.787	0.051	15.593	0.043	37.927	0.105
						F24	na	na	na	18.306	0.036	15.604	0.031	38.254	0.077
						F27	na	na	na	18.145	0.038	15.573	0.033	38.119	0.081
						F29	na	na	na	18.321	0.045	15.582	0.038	38.165	0.096
	101	Otter Sandstone Fm.	Anisian			1	115	0.020	0.021	18.417	0.049	15.819	0.028	38.972	0.199
						2	50.8	< 0.01	< 0.01	17.343	0.046	15.585	0.028	37.722	0.193
						3	23.6	0.046	0.020	18.426	0.049	15.742	0.028	38.549	0.200
						4	91.3	0.180	0.103	18.474	0.049	15.745	0.028	38.718	0.198
						F1	na	na	na	18.152	0.096	15.551	0.083	37.972	0.206
						F2	na	na	na	18.203	0.082	15.607	0.070	38.117	0.175
						F3	na	na	na	17.836	0.062	15.523	0.054	37.959	0.134
						F6	na	na	na	17.972	0.072	15.519	0.063	37.803	0.153
						F7	na	na	na	18.338	0.051	15.614	0.043	38.255	0.107
						F8	na	na	na	18.287	0.051	15.585	0.043	38.182	0.107
						F11	na	na	na	18.245	0.051	15.542	0.044	38.024	0.108
						F12	na	na	na	18.296	0.049	15.589	0.043	38.193	0.105
						F13	na	na	na	18.421	0.070	15.622	0.059	38.293	0.148
						F15	na	na	na	18.299	0.063	15.601	0.054	38.231	0.134
						F16	na	na	na	18.009	0.102	15.525	0.088	37.883	0.215
						F17	na	na	na	17.976	0.085	15.668	0.075	37.980	0.183
						F19	na	na	na	18.320	0.067	15.565	0.057	38.145	0.142
						F24	na	na	na	18.247	0.052	15.498	0.045	37.966	0.110
						F25	na	na	na	18.221	0.103	15.473	0.090	37.916	0.220
						F28	na	na	na	17.426	0.061	15.378	0.055	37.218	0.134
						F29	na	na	na	18.222	0.109	15.544	0.092	38.038	0.230
						F30	na	na	na	18.294	0.039	15.623	0.033	38.249	0.083
						F32	na	na	na	17.153	0.056	15.401	0.051	37.119	0.124
	102	Otter Sandstone Fm.	Anisian			1	na	na	na	18.462	0.041	15.685	0.025	38.605	0.192
						2	na	na	na	18.335	0.043	15.681	0.027	38.603	0.202
						3	na	na	na	18.333	0.040	15.621	0.025	38.382	0.191
						6	na	na	na	18.056	0.047	15.570	0.029	38.011	0.217
						F1	na	na	na	17.474	0.082	15.418	0.073	37.372	0.177
						F2	na	na	na	18.281	0.128	15.622	0.111	37.966	0.269
						F3	na	na	na	18.409	0.051	15.613	0.043	38.278	0.107
						F4	na	na	na	18.168	0.047	15.564	0.041	38.006	0.100
						F5	na	na	na	18.389	0.037	15.569	0.029	38.277	0.073
						F6	na	na	na	18.043	0.064	15.574	0.049	37.950	0.124
						F7	na	na	na	18.337	0.086	15.606	0.073	38.228	0.182
						F8	na	na	na	17.778	0.055	15.530	0.048	37.758	0.118
						F9	na	na	na	17.393	0.073	15.355	0.065	37.198	0.157
						F10	na	na	na	18.362	0.049	15.561	0.042	38.175	0.104
						F11	na	na	na	18.184	0.057	15.567	0.049	38.011	0.122
						F12	na	na	na	18.246	0.070	15.505	0.059	38.000	0.148
						F13	na	na	na	18.272	0.044	15.571	0.038	38.122	0.093
						F14	na	na	na	18.451	0.064	15.624	0.055	38.345	0.136
						F15	na	na	na	18.235	0.052	15.604	0.045	38.132	0.111
						F16	na	na	na	18.483	0.048	15.723	0.041	38.490	0.101
						F18	na	na	na	18.455	0.047	15.627	0.040	38.358	0.100
						F20	na	na	na	17.552	0.065	15.470	0.057	37.495	0.142
						F21	na	na	na	17.457	0.042	15.436	0.038	37.370	0.093
						F22	na	na	na	18.445	0.070	15.646	0.059	38.365	0.148
						F23	na	na	na	18.409	0.076	15.771	0.065	38.524	0.161
						F25	na	na	na	18.341	0.061	15.596	0.053	38.220	0.131
						F26 (Repeat 1)	na	na	na	18.461	0.068	15.657	0.058	38.407	0.144
						F27	na	na	na	18.232	0.042	15.621	0.036	38.161	0.090
						F28	na	na	na	17.556	0.056	15.514	0.050	37.582	0.121
	103	Otter Sandstone Fm.	Anisian			2	na	na	na	18.319	0.024	15.620	0.018	38.303	0.113
						3	na	na	na	18.352	0.028	15.614	0.020	38.237	0.134
						5	na	na	na	18.379	0.032	15.622	0.024	38.348	0.149
						6	na	na	na	18.292	0.028	15.546	0.022	38.170	0.131
	107	Otter Sandstone Fm.	Anisian			1	na	na	na	18.514	0.034	15.817	0.023	38.754	0.145
						2	na	na	na	18.458	0.033	15.565	0.022	38.305	0.143
						3	na	na	na	18.561	0.033	15.601	0.021	38.567	0.147
						4	na	na	na	17.124	0.031	15.314	0.024	37.006	0.145
						5	na	na	na	17.389	0.029	15.607	0.023	37.575	0.141
						7	na	na	na	17.611	0.025	15.590	0.018	37.927	0.116
						F1	na	na	na	18.166	0.045	15.542	0.039	37.966	0.096
						F2	na	na	na	18.290	0.029	15.583	0.024	38.141	0.061
						F3	na	na	na	18.218	0.034	15.546	0.029	38.057	0.071
						F5	na	na	na	18.167	0.036	15.563	0.031	38.005	0.076
						F6	na	na	na	18.232	0.032	15.551	0.028	38.096	0.068
						F8	na	na	na	18.235	0.032	15.549	0.027	38.086	0.068
						F9	na	na	na	18.299	0.053	15.565	0.045	38.114	0.112
						F10	na	na	na	18.253	0.033	15.645	0.029	38.257	0.071
						F11	na	na	na	18.304	0.044	15.593	0.037	38.213	0.093
						F12	na	na	na	18.244	0.047	15.534	0.041	38.017	0.101
						F13	na	na	na	17.470	0.034	15.341	0.030	37.087	0.074
						F14	na	na	na	17.899	0.037	15.403	0.032	37.589	0.079
						F15	na	na	na	18.172	0.044	15.346	0.038	37.491	0.094
						F16 (Repeat 4)	na	na	na	17.699	0.048	15.201	0.040	36.630	0.098
						F18	na	na	na	18.237	0.063	15.628	0.055	38.179	0.134
						F19 (Repeat 5)	na	na	na	17.477	0.068	15.590	0.061	37.628	0.147
						F20	na	na	na	17.837	0.058	15.587	0.050	37.772	0.125
						F21	na	na	na	18.346	0.043	15.638	0.037	38.301	0.091
						F22	na	na	na	17.560	0.036	15.535	0.032	37.591	0.078
						F23	na	na	na	18.183	0.059	15.650	0.052	38.181	0.126
						F24	na	na	na	18.165	0.055	15.550	0.047	37.993	0.118
						F25	na	na	na	18.319	0.030	15.567	0.026	38.156	0.065
						F26	na	na	na	17.397	0.124	15.420	0.111	37.129	0.270
						F27	na	na	na	18.230	0.045	15.585	0.039	38.180	0.097
	88S	Budleigh Salteron Pebble Beds	Clenekian	Clast of feldspar porphry		1	na	na	na	18.059	0.065	15.747	0.050	38.107	0.286
						2	na	na	na	18.039	0.044	15.607	0.034	37.821	0.221

* F denotes grain analysed using faraday collector configuration, all other grains analysed using ion counter collector configuration

Table 2: New Pb isotopic K-feldspar data from crysalline basement rocks in northern France, Cornwall and southeast Ireland, a
Lower Carboniferous sandstones in NW Ireland.

Unit Name	Location	Age	Grain	$^{206}Pb/^{204}Pb$	2σ	$^{207}Pb/^{204}Pb$	2σ	$^{208}Pb/^{204}Pb$
Barfleur Granite	Near Barfleur, Normandy, Northern France	Variscan	F1	18.240	0.047	15.528	0.040	38.008
			F2	18.198	0.097	15.499	0.083	37.931
			F3	18.316	0.051	15.602	0.044	38.192
			F4	18.306	0.053	15.591	0.045	38.170
			F5	18.281	0.073	15.581	0.063	38.156
Carolles Granite	Cliff below tower, Carolles, Normandy, Northern France	Cadomian	F1	17.495	0.054	15.483	0.048	37.461
			F2	17.484	0.053	15.456	0.047	37.435
			F3	17.621	0.082	15.598	0.072	37.759
Flamanville Granite	Anse De Sciotot, Normandy, Northern France	Variscan	F1	18.275	0.079	15.573	0.068	38.087
			F3	18.304	0.056	15.606	0.048	38.157
Leinster Granite	Dalkey Quarry, Co. Dublin, Ireland	Caledonian	F2	18.135	0.080	15.612	0.070	38.076
			F3	18.144	0.045	15.623	0.039	38.095
Brech granite	Near Brech, Brittany, Northern France	Variscan	F1	18.192	0.048	15.608	0.041	38.220
			F2	18.159	0.055	15.583	0.047	38.156
			F4	18.195	0.060	15.613	0.051	38.234
			F5	18.217	0.068	15.633	0.058	38.272
Lands End Granite	Cape Cornwall, SW United Kingdom		F1	18.388	0.038	15.597	0.032	38.277
			F2	18.408	0.139	15.591	0.118	38.270
			F3	18.535	0.102	15.715	0.088	38.553
			F4	18.470	0.087	15.642	0.074	38.425
			F5	18.469	0.105	15.668	0.090	38.437
Leinster Granite	Wicklow Gap, Co. Wicklow, Ireland	Caledonian	F1	18.190	0.052	15.609	0.045	38.072
			F2	18.157	0.030	15.575	0.026	37.992
			F3	18.275	0.036	15.647	0.031	38.196
			F4	18.173	0.025	15.582	0.021	38.009
Carnsore Granite	Carnsore Point, Co. Wexford,	Caledonian	F1	17.603	0.023	15.500	0.019	37.156

	Ireland		F2	17.587	0.022	15.467	0.011	37.089
			F3	17.541	0.015	15.473	0.010	37.092
Mylonitised vein cutting Kilmore Quay Group	Kilmore Quay, Co. Wexford, Ireland	?Precambrian	F1	18.423	0.070	15.713	0.061	38.302
			F2	18.422	0.047	15.715	0.039	38.288
			F3	18.116	0.075	15.392	0.066	37.490
			F4	18.246	0.060	15.615	0.050	38.019
			F5	18.146	0.069	15.515	0.064	37.756
			F6	18.219	0.081	15.407	0.069	37.522
Mullaghmore Sandstone Formation	Mullaghmore strand, Co. Sligo, Ireland	Lower Carboniferous	F1	14.330	0.028	14.716	0.025	34.656
			F2	17.926	0.021	15.550	0.019	37.560
			F3	17.946	0.036	15.548	0.031	37.565
			F4	17.967	0.032	15.590	0.028	37.661
			F5	16.948	0.063	15.279	0.058	36.254
			F6	18.032	0.022	15.575	0.019	37.697
			F8	16.845	0.051	15.579	0.047	34.148
			F10	14.229	0.026	14.701	0.020	34.603
			F11	17.720	0.067	15.549	0.059	36.458
			F12	16.886	0.068	15.411	0.050	36.304
			F13	17.318	0.024	15.440	0.022	36.708
			F14	13.724	0.032	14.493	0.027	33.808
			F15	13.778	0.025	14.520	0.026	33.181
			F16	13.470	0.030	14.603	0.033	33.298
			F17	13.975	0.024	14.618	0.025	33.388
			F18	15.713	0.048	15.094	0.036	33.910
			F19	17.781	0.056	15.420	0.050	37.267
			F20	17.493	0.076	15.528	0.067	37.096
			F21	14.099	0.032	14.659	0.030	34.390
			F22	14.158	0.050	14.701	0.038	34.177

and

2σ
0.100
0.204
0.108
0.110
0.156
0.117
0.114
0.178
0.167
0.120
0.173
0.095
0.102
0.116
0.127
0.145
0.080
0.293
0.216
0.184
0.222
0.110
0.064
0.077
0.052
0.045

0.028
0.024
0.149
0.097
0.162
0.123
0.151
0.170
0.061
0.046
0.075
0.069
0.135
0.047
0.104
0.050
0.140
0.128
0.052
0.065
0.061
0.076
0.059
0.093
0.121
0.159
0.072
0.094